JACS
JOURNAL OF THE AMERICAN CHEMICAL SOCIETY
pubs.acs.org/JACS
Article

Potassium Trimethylsilanolate-Promoted, Anhydrous Suzuki–Miyaura Cross-Coupling Reaction Proceeds via the "Boronate Mechanism": Evidence for the Alternative Fork in the Trail

Connor P. Delaney, Daniel P. Marron, Alexander S. Shved, Richard N. Zare, Robert M. Waymouth, and Scott E. Denmark*

Cite This: J. Am. Chem. Soc. 2022, 144, 4345–4364
Read Online
ACCESS | Metrics & More | Article Recommendations | Supporting Information

ABSTRACT: Previous studies have shown that the critical transmetalation step in the Suzuki–Miyaura cross-coupling proceeds through a mechanism wherein an arylpalladium hydroxide complex reacts with an aryl boronic acid, termed the oxo-palladium pathway. Moreover, these same studies have established that the reaction between an aryl boronate and an arylpalladium halide complex (the boronate pathway) is prohibitively slow. Herein, studies on isolated intermediates, along with kinetic analysis, have demonstrated that the Suzuki–Miyaura reaction promoted by potassium trimethylsilanolate (TMSOK) proceeds through the boronate pathway, in contrast with other, established systems. Furthermore, an unprecedented, binuclear palladium(I) complex containing a μ-phenyl bridging ligand was characterized by NMR spectroscopy, mass spectrometry, and computational methods. Density functional theory (DFT) calculations suggest that the binuclear complex exhibits an open-shell ground electronic state, and reaction kinetics implicate the complex in the catalytic cycle. These results expand the breadth of potential mechanisms by which the Suzuki–Miyaura reaction can occur, and the novel binuclear palladium complex discovered has broad implications for palladium-mediated cross-coupling reactions of aryl halides.

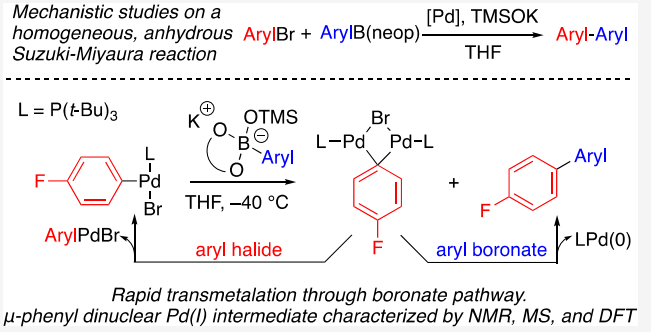

1. INTRODUCTION

The development of transition-metal-catalyzed, cross-coupling reactions has fundamentally changed the way chemists construct C–C bonds.[1] Because the formation of C–C bonds is central to synthetic organic chemistry, cross-coupling reactions are routinely applied in nearly every field in which organic chemistry is relevant, including polymer and materials chemistry,[2] medicinal chemistry,[3] small-molecule synthesis performed on small[4] and large scales,[5] and natural product synthesis.[6] The widespread impact of this technology was recognized by the 2010 Nobel Prize in Chemistry, awarded to Richard Heck, Ei-ichi Negishi, and Akira Suzuki for their pioneering studies on cross-coupling reactions.[1,7] Among cross-coupling reactions that form C–C bonds, the Suzuki–Miyaura cross-coupling[8] has emerged as the most powerful method—this fact is reflected in its status as the most commonly used C–C bond-forming reaction in the pharmaceutical industry.[1,3a]

Given the importance of the Suzuki–Miyaura reaction, the mechanism by which it proceeds is of considerable interest, as mechanistic understanding allows chemists to better optimize the process. At the most basic level, the Suzuki–Miyaura reaction involves three steps—oxidative addition, transmetalation, and reductive elimination.[9] Following advances in ligand design, transmetalation is frequently implicated as the turnover-limiting step in the Suzuki–Miyaura reaction, and therefore, the mechanism of transmetalation is particularly important.[8f,10] It has long been hypothesized that transmetalation in the Suzuki–Miyaura reaction proceeds through the intermediacy of a Pd–O–B-linked intermediate, with an oxyanionic base acting as a bridge between palladium and boron.[11] However, the mechanism by which such a Pd–O–B-linked species is formed has been the subject of much debate.[10] The two common hypotheses for the mechanism of Pd–O–B formation are termed the boronate pathway (path A) and the oxo-palladium pathway (path B) (Scheme 1).[12] In the boronate pathway, a 4-coordinate, 8-electron boronate species (8-B-4)[13] reacts with an arylpalladium halide complex, displacing the halogen and forming the pretransmetalation intermediate. In the oxo-palladium pathway, the arylpalladium

Received: August 9, 2021
Published: March 1, 2022

https://doi.org/10.1021/jacs.1c08283
J. Am. Chem. Soc. 2022, 144, 4345–4364

Scheme 1. Pretransmetalation Pathways in the Suzuki–Miyaura Reaction

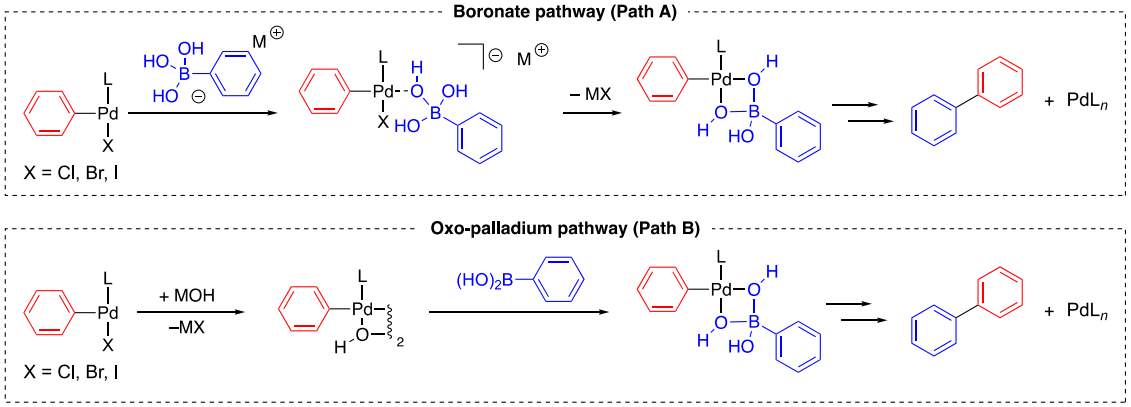

Scheme 2. Mechanistic Experiments by Amatore, Jutand, and Le Duc That Support Transmetalation through the Oxo-Palladium Pathway[14]

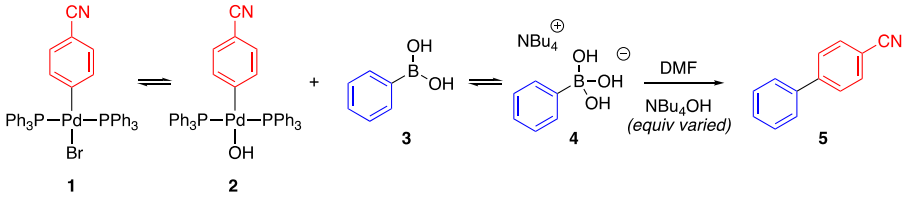

mol fraction **3**	k_{rel}
0.65	1
0.35	6
0	0.66

halide complex first undergoes an exchange with a base in solution to form an arylpalladium hydroxide complex that often spontaneously dimerizes. The resulting arylpalladium hydroxide dimer then reacts with a 6-electron, 3-coordinate boron compound (6-B-3), forming the same pretransmetalation intermediate (Scheme 1).

Studies that seek to differentiate between the boronate and oxo-palladium pathways are often hampered by heterogeneous reaction conditions originating from either (1) the biphasic aqueous/organic mixture typically employed in Suzuki–Miyaura reactions or (2) the insolubility of boronate salts in commonly used organic solvents. Despite these challenges, several experimental studies have demonstrated that the oxo-palladium pathway is operative in most Suzuki–Miyaura reactions. In one such study conducted by Amatore, Jutand, and Le Duc, the dependence of reaction rate on the concentration of boronic acid and tetrabutylammonium hydroxide was cited as evidence for an oxo-palladium mechanism (Scheme 2).[14] At low base concentration, a positive rate dependence on the mole fraction of boronate was observed. However, as the mole fraction of boronate approaches unity, the rate of reaction slows. Amatore, Jutand, and Le Duc hypothesize that the rate initially increases with the concentration of boronate because the base is needed to promote the formation of arylpalladium hydroxide complex **2**. However, as more base is added, the increased conversion of competent, 6-B-3 boronic acid **3** into incompetent 8-B-4 boronate species **4** causes the rate of reaction to decrease.

In another definitive study, Hartwig and Carrow directly compared the reactivities of catalytic intermediates implicated in the oxo-palladium and boronate pathways (Scheme 3).[12] The rate of transmetalation through the boronate pathway was determined by combining bis(triphenylphosphine)-arylpalladium halide complex **6** with potassium boronate **7** in the presence of 18-crown-6, and the rate of reaction to form biaryl **8** was measured. To explore the oxo-palladium pathway,

Scheme 3. Mechanistic Experiments from Hartwig and Carrow That Support Transmetalation through the Oxo-Palladium Pathway[12]

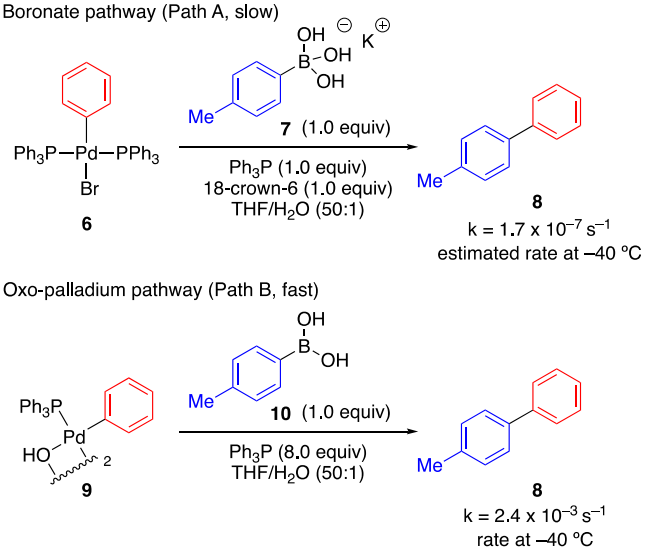

triphenylphosphine-ligated arylpalladium hydroxide dimer **9** was mixed with aryl boronic acid **10**. Hartwig and Carrow found that the oxo-palladium pathway kinetically outpaced the boronate pathway by several orders of magnitude.

In contrast, examples of transmetalation through the boronate pathway are rare. Matos and Soderquist found that alkylboranes transmetalate through the boronate pathway.[11] Computational studies by Ortuño, Lledós, Maseras, and Ujaque further suggest that the boronate pathway may be viable in some Suzuki–Miyaura reactions that cross-couple boronic acids.[15] Finally, Lima, Rodrigues, Silva, Silva, and Santos use competition experiments to support a boronate mechanism for the Suzuki–Miyaura reaction.[16]

https://doi.org/10.1021/jacs.1c08283
J. Am. Chem. Soc. 2022, 144, 4345–4364

2. BACKGROUND

2.1. Influence of Boronic Ester Structure on Boron-to-Palladium Transmetalation Rate. Although the intermediacy of Pd−O−B-linked pretransmetalation intermediates in the Suzuki−Miyaura reaction has long been hypothesized, no such complex had been identified or characterized until 2016, when Denmark and Thomas used their rapid-injection NMR (RI-NMR) apparatus[17] to generate and spectroscopically characterize the pretransmetalation intermediates in the Suzuki−Miyaura reaction.[18] During the course of that investigation, a Pd−O−B-linked complex incorporating a dimethyl boronic ester (**13**) was serendipitously discovered, characterized, and found to undergo transmetalation without prior hydrolysis to the boronic acid (Scheme 4).

Scheme 4. Serendipitous Discovery of Dimethyl Boronic Ester-Containing Pretransmetalation Intermediate 13

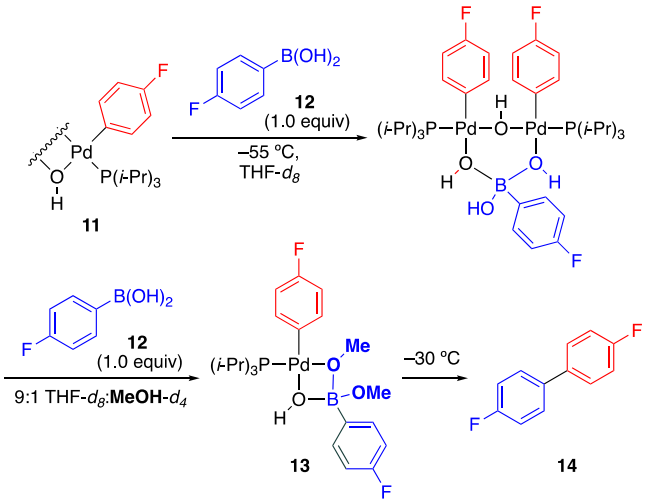

Following the successful formation of pretransmetalation intermediates that incorporate methyl boronic esters, it was logical to determine whether pretransmetalation intermediates could be formed that incorporate other boronic esters (Figure 1).[19] The combination of catechol boronic ester **15** with palladium hydroxide dimer **11** results in the formation of a new Pd−O−B intermediate incorporating the catechol ester. Likewise, a new Pd−O−B intermediate is formed when glycol boronic ester **16** is combined with **11**. Each complex was freshly formed and warmed to −30 °C, at which temperature transmetalation takes place. Interestingly, catechol ester **15** transmetalates 4× faster than boronic acid **12**, and both glycol ester **16** and dimethyl ester **17** react more than 20× faster than **12**. The observation that the boronic ester structure influences the rate of transmetalation suggests that the boronic ester structure can be used as a point of optimization alongside the ligand and precatalyst selection, which elevates boronic esters beyond their traditional use as protecting groups. For this insight to be of use, it is imperative to demonstrate that the rate increase can be harnessed in a preparative reaction. Thus, a method was developed to cross-couple boronic esters with the express intent of leveraging boronic ester identity to increase the reaction rate.

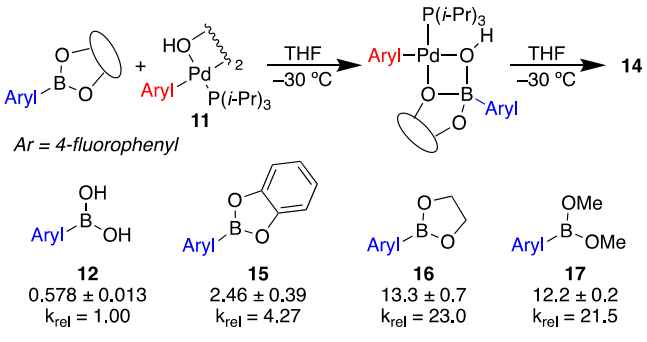

Figure 1. Enhanced rate of transmetalation in complexes incorporating boronic esters.

2.2. Development of an Anhydrous, Homogeneous, Suzuki−Miyaura Cross-Coupling of Boronic Esters. To develop the aforementioned method, it was decided that anhydrous reaction conditions would be optimal to prevent undesired ester hydrolysis. However, initial investigations using inorganic bases commonly employed in Suzuki−Miyaura reactions were hampered by the insolubility of these bases in aprotic solvents. Inspired by prior work in the Denmark laboratory on cross-coupling reactions of organosilicon reagents,[20] potassium trimethylsilanolate (TMSOK) was identified as a base to promote the homogeneous, anhydrous Suzuki−Miyaura cross-coupling of boronic esters (Scheme 5).

Scheme 5. Homogeneous, Anhydrous Suzuki−Miyaura Reaction Promoted by TMSOK[21]

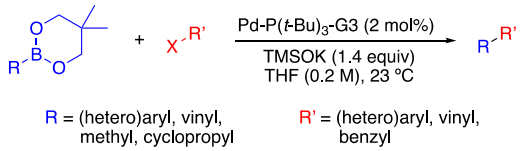

It was demonstrated that the reaction time for several example reactions could be shortened from days to hours, without changing the ligand or precatalyst, simply by employing an appropriate boronic ester as the nucleophile, TMSOK as the base, and anhydrous ethereal as solvent.[21] The homogeneous, anhydrous reaction conditions have also been adapted to the cross-coupling of heteroaryl nucleophiles with heteroaryl electrophiles, wherein the use of aqueous conditions can facilitate protodeboronation.[22,23]

As mentioned previously, the Suzuki−Miyaura reaction is frequently carried out using boronate complexes that are poorly soluble in organic media. In contrast, TMSOK-ligated boronates are highly soluble in tetrahydrofuran (THF). It was of interest to uncover what effect a soluble boronate has on the reaction mechanism, particularly with regard to the formation of a Pd−O−B intermediate. Furthermore, an explanation was sought for an anomaly uncovered during reaction optimization, namely, a stark dependence of product yield on base stoichiometry was observed. As the concentration of base exceeds the concentration of boronic ester, the reaction rate drops precipitously, with <30% yield observed when using 2.0 equiv or more base.[21] Finally, the structure of the Pd−O−B-linked intermediate was of interest, given that TMSOK is a much poorer bridging ligand than hydroxide. With that in mind, the following goals were identified for this study:

1. Determine what mechanistic features lead to the observed dependence of reaction rate on base stoichiometry,

https://doi.org/10.1021/jacs.1c08283
J. Am. Chem. Soc. 2022, 144, 4345−4364

2. Identify pretransmetalation intermediates incorporating TMSOK and neopentyl boronic esters, and
3. Determine if transmetalation proceeds through a boronate or oxo-palladium mechanism.

3. RESULTS

3.1. Stoichiometric Experiments Probing the Mechanism of Transmetalation. *3.1.1. Experimental Design.* Three potential transmetalation mechanisms were explored by studying reactions of isolated catalytic intermediates (Scheme 6)—the boronate pathway (path A), the oxo-palladium pathway (path B), and a third scenario termed path C, wherein a molecule of boronate reacts with an arylpalladium silanolate complex. First, reactivity through the boronate pathway (path A) was explored by combining a TMSOK-ligated, 8-B-4 boron reagent with an arylpalladium halide complex and observing the resulting reactivity. Second, the oxo-palladium pathway (path B) was explored by attempting to generate an arylpalladium silanolate complex and then combine it with a 6-B-3 boronic ester. Finally, path C was investigated by combining an arylpalladium silanolate complex with 8-B-4 boronate. In each case, the reaction was monitored using ^{19}F NMR spectroscopy, allowing for the detection of any new species formed while simultaneously monitoring the concentration of the various species in solution.

Scheme 6. Three Proposed Reaction Pathways That Were Investigated

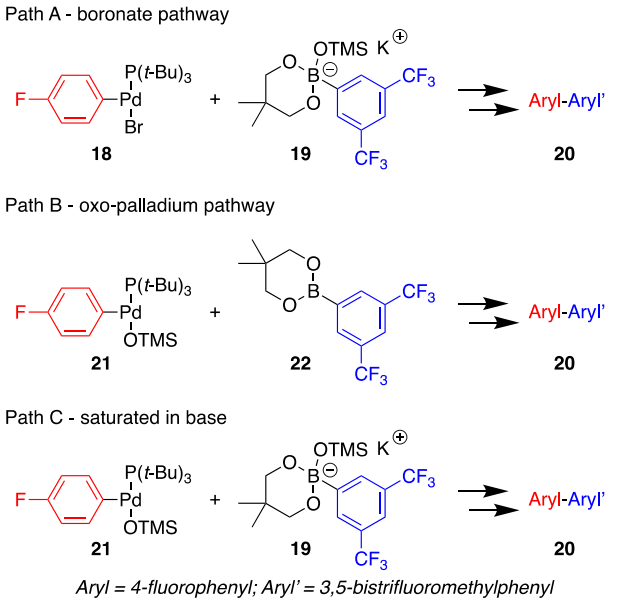

Aryl = 4-fluorophenyl; Aryl' = 3,5-bistrifluoromethylphenyl

3.1.2. Investigation of Transmetalation through the Boronate Pathway. To test the boronate pathway (path A), 4-F-C_6H_4Pd[P(*t*-Bu)$_3$]Br (**18**) was combined with 1.0 equiv of TMSOK-ligated boronate complex of neopentyl 3,5-bistrifluoromethylphenylboronic ester (**19**) at −40 °C in THF. The combined reagents readily reacted at −40 °C to ultimately generate biaryl **20** following transmetalation and reductive elimination (Figure 2). No pretransmetalation complex was observed, implying that the reaction is either intermolecular, that binding of boronate to the palladium complex is rate-determining, or that the reaction follows Michaelis−Menten kinetics with a large value of K_M.

The concentration of various species in the reaction mixture was monitored over the course of 23 min at −40 °C using ^{19}F NMR spectroscopy. After 23 min, all of palladium complex **18** had been consumed, but the concentration of biaryl product **20** was lower than expected and boronate **19** was only partially consumed. Furthermore, a new, unidentified species (**23**) characterized by a ^{19}F NMR signal at −127.5 ppm was formed alongside the biaryl product **20**.

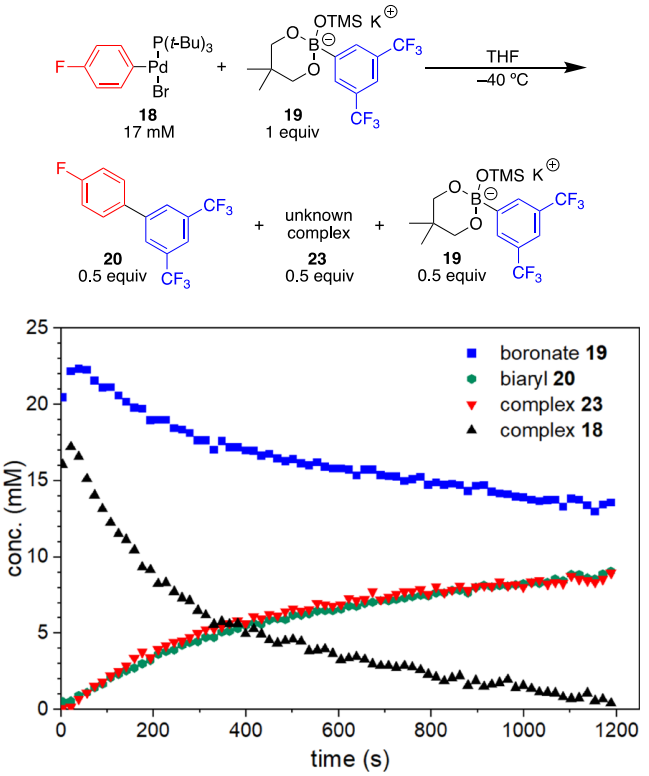

Figure 2. Plot of the concentration of reaction components vs time during transmetalation through the boronate pathway.

The observation that boronate complex **19** reacts with Pd complex **18** to form biaryl **20** at −40 °C demonstrates that transmetalation through the boronate pathway is kinetically accessible in this system. This observation stands in contrast to prior results obtained using boronic acids under Hartwig and Carrow's reaction conditions, in which the boronate pathway was prohibitively slow.[12] The high rate of transmetalation at −40 °C is also noteworthy. However, these findings were complicated by the appearance of species **23**. Examining the reaction stoichiometry revealed that for each equiv of boronate **19** consumed, 2 equiv of Pd complex **18** was consumed. Correspondingly, 1 equiv of biaryl product **20** and 1 equiv of unknown **23** were formed.

In view of the observed stoichiometry and the consistently equimolar concentration of **20** and **23** over time (Figure 2), it was hypothesized that unknown complex **23** could be formed through a reaction between a post-reductive elimination reaction byproduct and the arylpalladium halide complex **18**. With biaryl **20** accounted for in the ^{19}F NMR spectrum, possible candidates for this reaction byproduct are P(*t*-Bu)$_3$Pd(0) (**24**) and boron byproduct **25** (Figure 3). To further elucidate the structure of the unidentified complex, it was characterized using a variety of 1-D and 2-D NMR spectroscopy techniques.

https://doi.org/10.1021/jacs.1c08283
J. Am. Chem. Soc. 2022, 144, 4345−4364

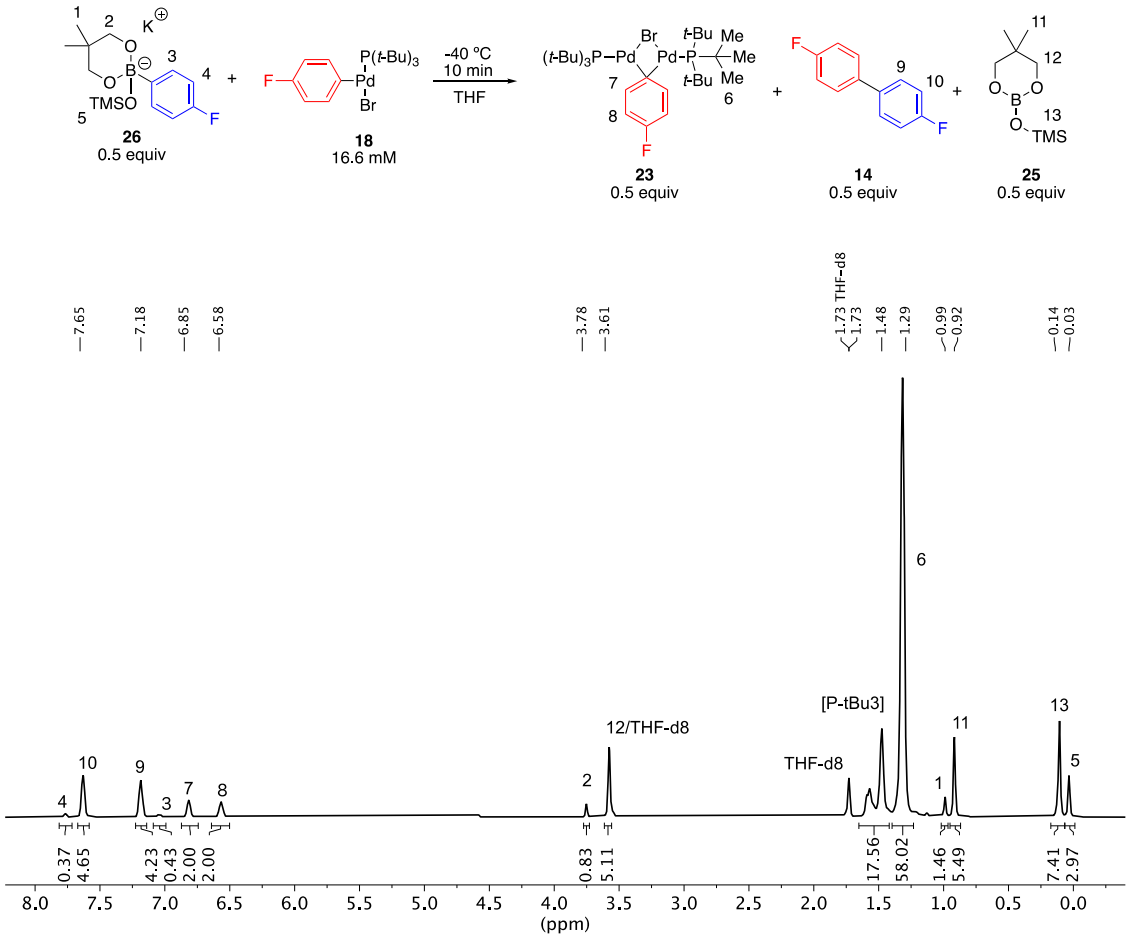

Figure 3. ^{1}H NMR spectrum of unknown species 23, biaryl 14, and boron byproduct **25**.

*3.1.3. Characterization of Unknown **23** through NMR Spectroscopy.* Attempts to isolate complex **23** were unsuccessful, as it was observed to decompose at temperatures above −10 °C. Instead, a fresh sample was generated in situ, and spectroscopic characterization of the new complex **23** as a component of the product mixture was performed by means of ^{1}H, ^{19}F, ^{31}P, and ^{13}C NMR spectroscopies alongside 2-D experiments including COSY, ROESY, HSQC, and HMBC. The boronate reagent used to synthesize **23** does not appear to influence the structure or yield of the product complex. Spectra of **23** generated by a combination of arylpalladium bromide **18** with boronate **26** were identical to those of **23** generated from **18** and boronate **19**, excepting the resonances associated with the biaryl product **14** or **20**. The ^{1}H spectrum shown in Figure 3 is of a reaction mixture wherein **26** was used as the boronate reagent.

In the aryl region of the ^{1}H NMR spectrum, resonances associated with biaryl **14** are observed at 7.65 and 7.18 ppm, integrating to four protons each. Two additional resonances at 6.85 and 6.58 ppm are assigned to the unknown complex. In the alkyl region, peaks consistent with boron byproduct **25** are observed at 3.61, 0.92, and 0.14 ppm. Finally, the singlet at 1.29 ppm integrating to 54 protons was assigned to two chemically equivalent P(*t*-Bu)$_3$ ligands. The chemical equivalence of the phosphine ligands is corroborated by the observation of one major peak at 77.3 ppm by ^{31}P NMR analysis. The remaining signals are assigned as a small quantity of residual **26**.

COSY, HSQC, and HMBC spectra were obtained for the mixture in THF-d_8 but were not structurally informative. However, the ROESY spectrum contained cross-peaks demonstrating polarization transfer between the P(*t*-Bu)$_3$ protons and both ortho and meta 4-F-C$_6$H$_4$ protons, suggesting that the ligand and arene are both part of one molecule and not two components of a mixture. Full characterization data are provided in the Supporting Information.

Taken together, these data suggest that the unknown complex contains a 4-fluorophenyl group and two symmetrically related tri-*tert*-butylphosphine groups. We hypothesize that such a complex could be produced if the highly reactive complex P(*t*-Bu)$_3$Pd(0) generated following reductive elimination combined with arylpalladium bromide complex **18** to form a new, binuclear palladium complex (Scheme 7). To further test this hypothesis, mass spectrometry was used to establish the composition of matter and gain further structural information.

*3.1.4. Mass Spectrometric Characterization of **23**.* The temperature sensitivity of complex **23** and the low dielectric constant of THF created several challenges in the characterization by mass spectrometry. We employed a modified pressurized sample infusion (PSI) air-free sampling technique developed by McIndoe[24] by modeling a cold electrospray ionization (CSI) apparatus developed by Yamaguchi et al.[25] to ensure that the reaction mixture could be maintained under an inert atmosphere below −20 °C until ions reached the gas

https://doi.org/10.1021/jacs.1c08283
J. Am. Chem. Soc. 2022, 144, 4345−4364

Scheme 7. Proposed Structure of Unknown 23 Characterized by ^{19}F Peak at −127.5 ppm

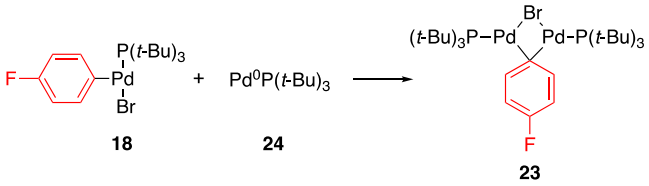

phase. The sampling apparatus and conditions for all MS experiments are detailed in the Supporting Information. As **23** had been previously generated and characterized in THF, a suboptimal solvent for electrospray ionization, we utilized ^{19}F NMR spectroscopy to confirm that complex **23**, once generated as a solution in THF, persisted through dilution with up to 50% of precooled acetonitrile. For the THF/CH_3CN experiments, complex **23** was prepared in THF as illustrated in Figure 3 and held for 30 min at −40 °C before being diluted with cold (−45 °C) acetonitrile and subsequently cooled to a sampling temperature of −78 °C.

Cold electrospray of complex **23** results in several ions containing one and two palladium atoms (Figure 4), clearly distinguished by their broad isotopic pattern. Ions in this discussion are annotated by their most abundant monoisotopic masses, and the composition of matter was confirmed for each assigned ion by matching the exact mass and observed isotopic pattern with simulated patterns. The most intense ion observed (m/z 713) matches the molecular formula $[C_{30}H_{58}FP_2Pd_2]^+$ (calculated: 713.2080 found: 713.2078), which is consistent with the ionization of complex **23** by the loss of a bromide ion. This bromide-loss ion (m/z 713) was also detected in pure THF, indicating that a bromide-loss ionization pathway does not require the presence of a high-dielectric solvent. However, in pure THF, the total signal intensity was quite poor and no bromide-retaining ions were detected, motivating the acquisition of all other spectra in a 1:3 mixture of MeCN and THF.

An additional, lower-intensity ion centered at m/z 791.1156 matches the elemental composition $[C_{30}H_{57}BrFP_2Pd_2]^+$ (calculated: 791.1177 found: 791.1156), which is consistent with the ionization of complex **23** by the loss of a hydride ion. We propose that such an ion may reasonably form during electrospray if the aryl ligand of **23** undergoes a C−H insertion to the adjacent Pd center, followed by hydride loss. The absence of an ion at m/z 791 in pure THF might be indicative of a solvent-dependent ionization pathway or simply a consequence of the low ion counts observed in THF.

We believe that this hydride elimination is a consequence of the high voltages applied in electrospray and therefore dependent on a high-dielectric solvent. The total intensity of ions around m/z 791 could be improved with more suitable electrospray solvents, but ^{19}F NMR experiments showed that higher concentrations of acetonitrile reduced the stability of the desired complex. This ion critically establishes the closest composition of matter to the proposed neutral complex **23**. The overlapping envelope centered at m/z 786.2244 remains unassigned despite our best efforts at characterization. The intensity of this overlapping peak was highly unstable between scans, and we suspect that it is a product of mild degradation or rearrangement of **23** during electrospray. Other multi-Pd peaks, possibly indicative of solvent-mediated clusters, are observed in electrospray ionization mass spectrometry (ESI-MS) spectra but none are sufficiently enlightening to be worthy of discussion.

The observation of ions with m/z 713 and m/z 791 in the cold electrospray ionization (CSI) experiments is consistent with the proposed structure of **23**. To provide further information on the structure and gas-phase reactivity of these unusual binuclear Pd complexes, we utilized high-energy collisional dissociation (HCD)[26] tandem mass spectrometry to generate fragment ions in the gas phase. In this technique, ions of interest are isolated in the C-trap of the Orbitrap XL mass spectrometer and accelerated into a dedicated octupole collision cell containing He bath gas. This MS^n technique has several advantages over more conventional collision-induced

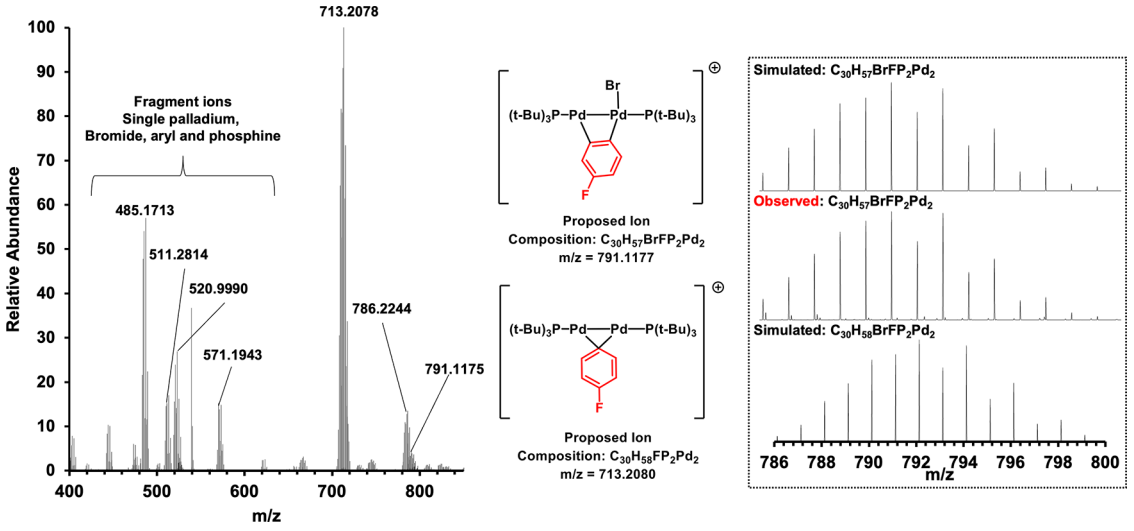

Figure 4. Left, mass spectrum resulting from the modified cold-spray ionization of complex **23** containing relevant species labeled above 10% abundance. Proposed structures of the notable ions are shown in the middle; other assignments may be found in the Supporting Information. Simulated peaks are shown at the far right, illustrating the distinctive multi-Pd isotopic pattern and positive confirmation of the peak at m/z 791.1175 matching the molecular formula of complex **23** minus a hydride equivalent. Simulated peaks are modeled as Gaussian distributions at a resolution of 60 000.

https://doi.org/10.1021/jacs.1c08283
J. Am. Chem. Soc. 2022, 144, 4345−4364

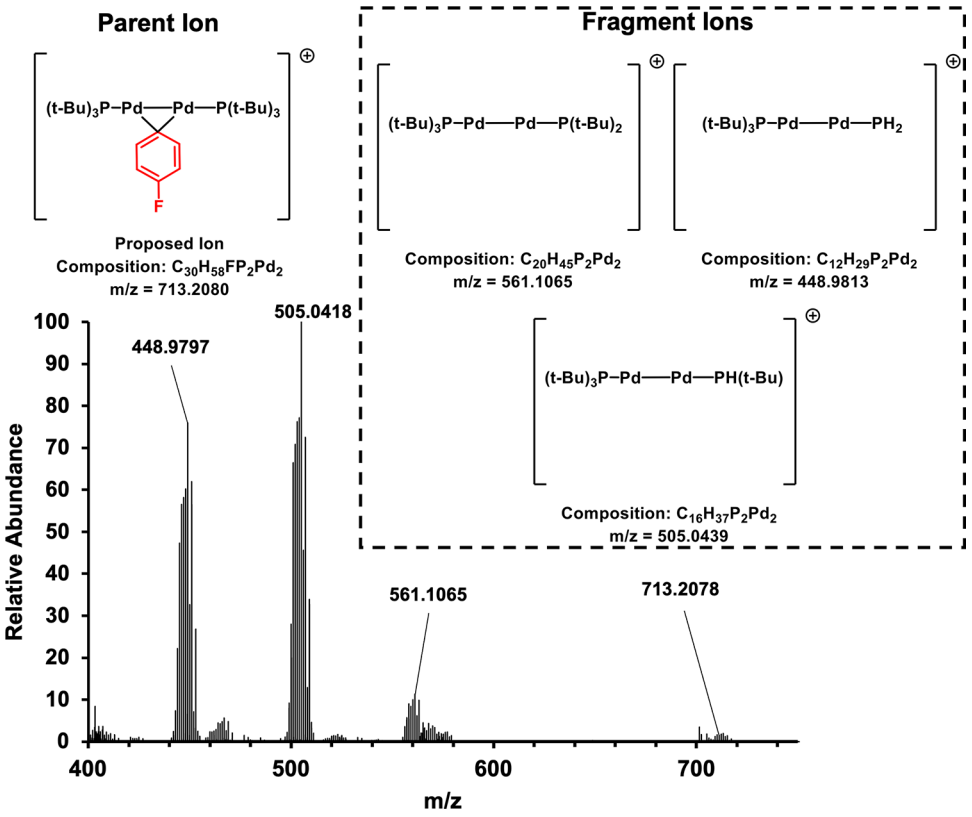

Figure 5. Fragments detected by tandem MS (HCD) treatment of ions centered at m/z 713.2078 (isolation range of 15 m/z). Proposed formulas were matched to peaks by a comparison of monoisotopic mass and isotopic pattern to simulated spectra.

dissociation (CID) experiments carried out in LTQ mass spectrometers. Ion-selection in the C-trap is more precise, and the lifetime of ions and collisional energies accessible in the octupole collision cell allows for both collisional dissociation and ion–molecule reactions that can provide rich information on the structure and reactivity of the selected ions. Further, the storage and transmission capacities of the C-trap are markedly higher than those of the LTQ, which proved critical in resolving the full isotopic pattern of multi-Pd ions.

Fragments resulting from the HCD treatment of the bromide-loss ion centered at m/z 713.2078 are shown in Figure 5. The sequential loss of isobutene via a McLafferty-type rearrangement confirms the presence of tri-*tert*-butylphosphine in each of the fragments, while the isotopic patterns definitively match dipalladium species. Fragmentation by HCD of the putatively bromide-containing ion centered at 791.1177 results in several fragment ions matching those in Figure 5, corroborating the relationship between the two species. Annotated HCD spectra for both ions can be found in the Supporting Information. In addition to features that confirm structural motifs, most of the observed fragment ions retain a Pd–Pd bond. These rearrangements after the loss of the bromide and aryl motifs suggest a surprisingly robust Pd–Pd bond, apparently ambivalent in the gas phase to the presence of bridging ligands.

Mass spectrometric data are consistent with the proposed structure of **23**, in both composition of matter and connectivity. Repeated low-temp and air-free MS observation and corroboration by ^{19}F NMR strongly support the structural assignment of the proposed binuclear arylpalladium bromide complex. Furthermore, the HCD experiments suggest the presence of a robust palladium–palladium bond that remains intact even as the various ligands are stripped from palladium.

3.1.5. Transmetalation and Oxidative Addition Reactions with Complex ***23****.* With strong evidence supporting the structural characterization of **23**, its reactivity was next explored. It was hypothesized that **23** could be competent to undergo both transmetalation, furnishing two palladium(0) complexes following reductive elimination, and oxidative addition, furnishing 2 equiv of arylpalladium(II) halide.

To explore whether transmetalation occurs when boronate **19** is combined with complex **23**, 1.0 equiv of oxidative addition complex **18** was combined with 1.0 equiv of boronate **19** in THF at −10 °C. After the reaction mixture was aged for 100 s at −10 °C, arylpalladium bromide complex **18** had reacted quantitatively with 0.5 equiv of boronate **19** to generate 0.5 equiv of complex **23** and 0.5 equiv of biaryl **20** (Figure 6). From this point, complex **23** and boronate **19** continued to react to form biaryl **20**, albeit at a substantially reduced rate.

Beginning with the time point at which the concentration of complex **23** is at a maximum, the stoichiometry of reaction was examined. For each equiv of boronate **19** consumed, 1 equiv of biaryl **20** is formed, suggesting quantitative conversion from boronate **19** to product **20**. However, an excess of complex **23** is consumed in the process. Given the observed instability of **23** at −10 °C (Section 3.1.3), it is likely that the excess consumption of complex **23** is the result of concurrent decomposition of the complex.

Next, the propensity of complex **23** to react with an aryl halide in an oxidative addition reaction was explored. First, 10 μmol of arylpalladium bromide complex **18** was combined with 0.5 equiv of boronate **26** in THF at −78 °C and then

https://doi.org/10.1021/jacs.1c08283
J. Am. Chem. Soc. 2022, 144, 4345−4364

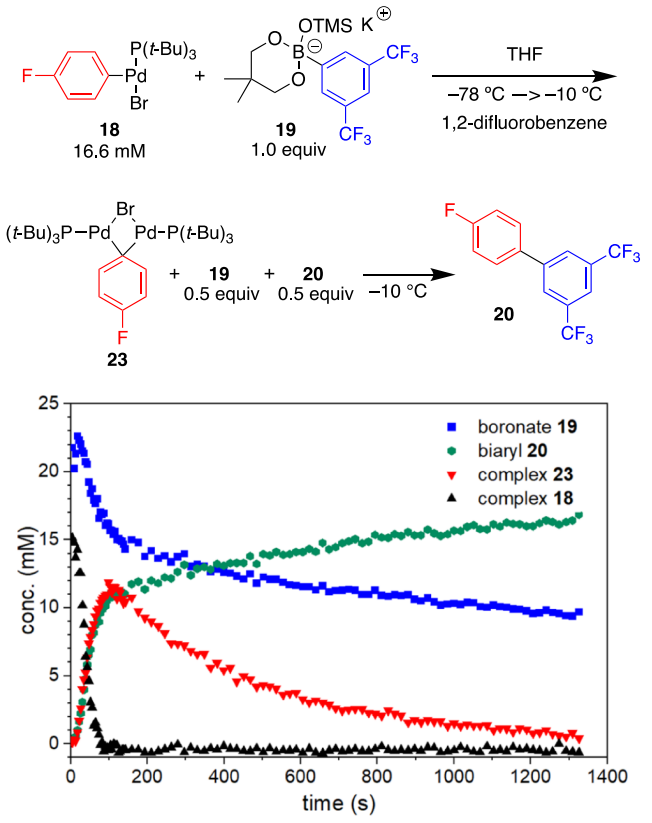

Figure 6. Path A transmetalation at −10 °C, showing further transmetalation from complex **23**.

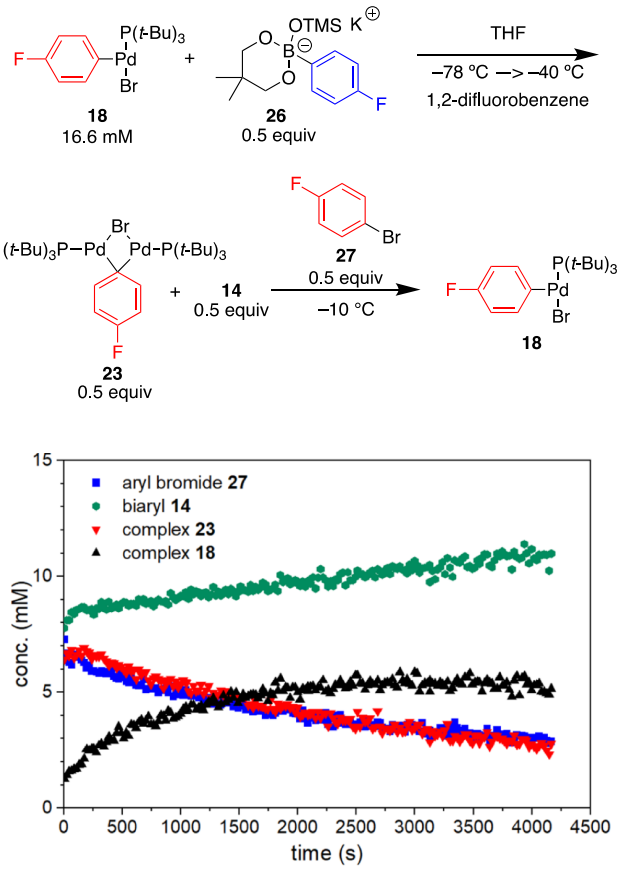

Figure 7. Conversion of complex **23** into oxidative addition complex **18** in the presence of aryl bromide **27**.

warmed to −40 °C to generate 5 μmol of **23** with complete consumption of **18** and **26**. The mixture was cooled to −78 °C, 5 μmol of aryl bromide **27** in THF was added to the solution of complex **23**, the mixture was warmed to −10 °C, and monitored by ^{19}F NMR spectroscopy (Figure 7). The concentration of complex **23** and aryl bromide **27** decreased over time, and the concentration of oxidative addition complex **18** increased over time. Furthermore, a small amount of biaryl product **14** was observed to form (Figure 7).

Once again, the change in the concentration of complex **23** and aryl bromide **27** was identical, suggesting that the two are reacting with 1:1 stoichiometry. For each equiv of aryl bromide **27** and complex **23** that are consumed, 1.3 equiv of arylpalladium halide complex **18** are generated. Furthermore, biaryl **14** is generated in substoichiometric quantities. The generation of biaryl **14** may be the result of decomposition of complex **23** or arylpalladium halide complex **18**.

In summary, complex **23** undergoes transmetalation and subsequent reductive elimination to form biaryl **20** when combined with boronate **19** and undergoes oxidative addition when combined with aryl bromide **27** to form arylpalladium halide complex **18**. Although neither reaction proceeds in quantitative yield, the decomposition of the relevant palladium species is a plausible explanation for the remainder of the mass balance. Altogether, these observations establish the reactivity of the new complex and further support the structural hypothesis put forward in Section 3.1.3.

3.1.6. Exploration of Transmetalation through Paths B and C. Having established the kinetic competence of the boronate pathway, the investigation continued by exploring whether the oxo-palladium pathway was also potentially operative. By combining 4-F-C_6H_4Pd[P(*t*-Bu)$_3$]OTMS (**21**) with neopentyl 3,5-bistrifluoromethylphenylboronic ester (**22**) at −40 °C, the competence of the oxo-palladium pathway could be tested. However, multiple species exhibiting broad resonances were observed when TMSOK and **18** were mixed in a 1:1 ratio in d_8-THF.[27] The collected data, discussed in the Supporting Information, suggest that 4-F-C_6H_4Pd[P(*t*-Bu)$_3$]-OTMS (**21**) may not exist as a well-defined compound at this concentration and temperature and that it may be in an equilibrium with free TMSOK and other palladium complexes. Only upon the addition of a second equivalent of TMSOK as a solution in d_8-THF did the speciation reconverge, resulting in a new species exhibiting a ^{19}F NMR resonance at −126 ppm (Scheme 8; see the Supporting Information for full characterization data).

Despite not having a well-defined method for the generation of 4-F-C_6H_4Pd[P(*t*-Bu)$_3$]OTMS (**21**), the reaction between putative complex **21** and neopentyl 3,5-bistrifluoromethylphenylboronic ester (**22**) was investigated (Scheme 9). First, 1.0 equiv of a THF solution of TMSOK was added to a THF

Scheme 8. Reaction Between 18 and 1 or 2 Equiv of TMSOK

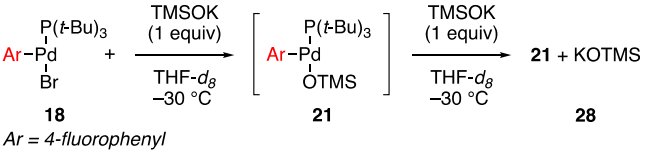

https://doi.org/10.1021/jacs.1c08283
J. Am. Chem. Soc. 2022, 144, 4345−4364

solution of arylpalladium bromide complex **18** in a 5 mm NMR tube held at −78 °C. Next, a THF solution containing 1.0 equiv of neopentyl 3,5-bistrifluoromethylphenylboronic ester **22** was added at −78 °C, the mixture was inserted into an NMR magnet precooled to −40 °C, and the evolution of species over time was monitored by ^{19}F NMR spectroscopy.

At t = 0 s, the biaryl product **20** had already been formed at a concentration of ca. 4 mM, corresponding to a roughly 25% yield w.r.t. the initial arylpalladium halide complex **18**. Also present was 8-B-4 boronate **19**, present in 8 mM concentration, alongside several species containing palladium, which are discussed in more detail in the Supporting Information. The system was monitored at −40 °C for 20 min, but no further change in the concentration of **19** or **20** was observed.

Scheme 9. Experiment Designed to Probe Transmetalation through the Oxo-Palladium Pathway

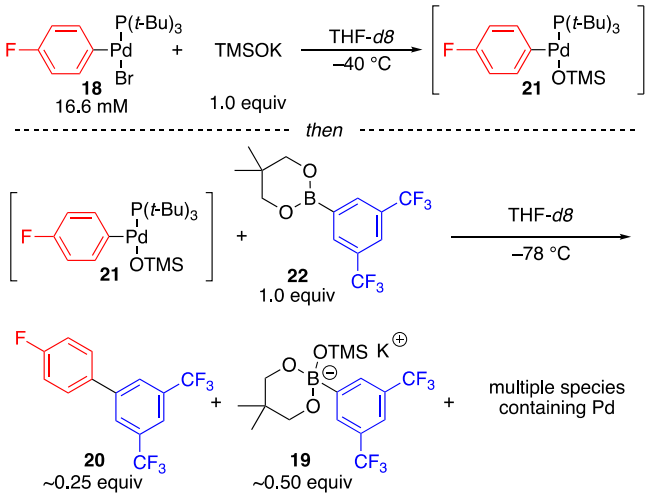

These results are not compelling; determination of the reaction rate law (*vide infra*) ultimately furnished more conclusive evidence against transmetalation through the oxo-palladium pathway (path B). Nonetheless, several inferences can be made from these data. First, the oxo-palladium pathway may be very fast, given that the biaryl product was formed prior to the acquisition of spectra at −40 °C. However, the inability to characterize arylpalladium−OTMS complex **21** as a discrete intermediate suggests that KOTMS may not displace bromide from the palladium complex. The generation of 8-B-4 boronate **19** from the mixture of putative arylpalladium silanolate complex **21** and 6-B-3 ester **22** further supports the notion that the binding affinity of TMSOK toward boronic ester **22** is much greater than its affinity toward palladium complex **18**. The earlier two observations, in concert with kinetic evidence refuting transmetalation through the oxo-palladium mechanism in this system (*vide infra*), suggest that even if the barrier to the reaction between **21** and **22** is low, the speciation in solution may render the oxo-palladium mechanism inoperative. An expanded discussion of the investigation into transmetalation through the oxo-palladium pathway is included in the Supporting Information.

Finally, an experiment was carried out to study transmetalation in the presence of excess TMSOK (path C). First, 4-F-C_6H_4Pd[P(t-Bu)$_3$]Br (**18**) was mixed with 3.0 equiv of TMSOK in THF at −78 °C to generate a new complex, as shown in Scheme 8. Next, a THF solution of 1.0 equiv of neopentyl ester **22** was added at −78 °C. The neopentyl ester rapidly reacted with TMSOK to form boronate **19** in situ. The reaction mixture containing 1.0 equiv 4-F-C_6H_4Pd[P(t-Bu)$_3$]-OTMS (**21**), 1.0 equiv boronate **18**, and 1.0 equiv TMSOK in THF was lowered into an NMR magnet precooled to −40 °C, and the evolution of species over time was monitored using ^{19}F NMR spectroscopy. No changes were observed over the course of 20 min. The magnet was warmed to −10 °C and again monitored by ^{19}F NMR spectroscopy, and no change was observed over the course of 20 min. Finally, the NMR magnet was warmed to 10 °C, at which temperature **28** decomposed without conversion to biaryl **20**. Clearly, the palladium complex formed in the presence of an excess of free TMSOK is not competent to undergo transmetalation with boronate **18**. These data suggest that the path C reaction mechanism is not viable, which is in good agreement with the dependence of reaction yield on base stoichiometry and prior results obtained by Amatore, Jutand, and Le Duc.[14]

3.1.7. Summary of Results from Stoichiometric Reactions. In summary, the formation of a putative pretransmetalation intermediate through the boronate pathway (path A) is kinetically viable, and it leads to the generation of a heretofore unknown intermediate **23**. The reactivity and structural characterization data of **23** are consistent with the structural hypothesis put forward in Section 3.1.3. Attempts to characterize arylpalladium silanolate complex **21** showed the generation of new species with the consumption of arylpalladium halide complex **18**, but the lack of a single, discrete complex suggests that the binding between arylpalladium(II) and trimethylsilanolate is relatively weak compared to that between arylpalladium(II) and hydroxide. Experiments probing transmetalation through the oxo-palladium pathway (path B) were ultimately inconclusive. Finally, the lack of reactivity observed through path C offers an explanation for the relationship between base stoichiometry and reaction yield observed in the TMSOK-promoted Suzuki−Miyaura reaction. No new NMR resonances consistent with a Pd−O−B intermediate were observed, suggesting that if such an intermediate exists, it lies at the unfavorable end of an equilibrium or exists on the reaction coordinate after the turnover-limiting step.

Next, a rate equation for the TMSOK-promoted Suzuki−Miyaura reaction of neopentyl boronic esters was determined to identify the species that are involved between the resting state and turnover-limiting transition state. Furthermore, such experiments could reveal whether complex **23** represented an artifact of the stoichiometric reaction conditions or a relevant catalytic intermediate.

3.2. Kinetic Analysis of the TMSOK-Promoted, Suzuki−Miyaura Reaction. *3.2.1. Experimental Design.* The inconclusive results for path B in the previously described studies under stoichiometric conditions preclude the direct comparison of transmetalation rates through paths A and B. Determination of the rate equation through kinetic analysis could provide compelling evidence for which pathway is operative in the catalytic reaction.

Even when electron-deficient neopentyl 3,5-bistrifluoromethylphenylboronic ester (**22**) was used as the nucleophile with the intent to lower the reaction rate by decreasing the migratory aptitude of the migrating arene, the reaction was >50% complete in seconds at 22 °C. To allow for the collection of sufficient initial rate data for kinetic analysis,

https://doi.org/10.1021/jacs.1c08283
J. Am. Chem. Soc. 2022, 144, 4345−4364

reactions were performed at −25 °C. Arylpalladium halide complex **18** (from 4-fluorobromobenzene) was chosen as the palladium source, as it is assumed to be a competent catalytic species that does not require activation to enter the catalytic cycle.[28] For the electrophilic species, 4-bromofluorobenzene was chosen because fluoroarenes have a substantial dependence of ^{19}F chemical shift on the electronic environment, allowing for the identification and quantification of species by ^{19}F NMR spectroscopy.

Kinetics experiments were performed by premixing THF solutions of boronic ester **22**, aryl bromide **27**, arylpalladium halide complex **18**, and an internal standard in a 5 mm NMR tube, and then adding a solution of TMSOK in THF at −78 °C, with the reaction initiated by lowering the tube into an NMR magnet precooled to −25 °C. All experiments were performed in triplicate, and error bars represent the standard deviation of the triplicate rates. Partial reaction orders were determined using the method of initial rates. The mixture was allowed to age for 100 s to establish a steady state, and then the rate was measured as the slope of product formation vs time for 11 time points between 100 and 200 s. All partial reaction orders were determined by fitting the power function $y = k_{obs}[conc]^a$, where y represents the initial rate, k_{obs} represents the observed rate constant, [conc] represents the concentration of the reagent, and "a" represents the partial reaction order.

Because TMSOK reacts rapidly and completely with boronic ester **22** to form boronate **19**, the concentration of free TMSOK in all reactions is negligible. The concentration of TMSOK in the reaction cannot be independently controlled—changing the amount of TMSOK added to the reaction only changes the concentration of boronate **19** and boronic ester **22**. Free TMSOK in excess of boronic ester **22** severely inhibits the reaction (Section 3.1.6). As a result, the following kinetic investigation determines the reaction order for each major species in solution: aryl halide **27**, boronate **19**, boronic ester **22**, and palladium catalyst **18**.

3.2.2. Reaction Order in Aryl Halide 27. First, the partial reaction order in aryl halide was determined (Figure 8). Across an 8-fold range of concentrations, the partial reaction order in aryl bromide was found to be 0.49 ± 0.02. A dependence of rate on aryl bromide concentration precludes turnover-limiting transmetalation through either the boronate or oxo-palladium pathway. Furthermore, the fractional reaction order is consistent with a mechanism wherein a reversible dissociation of one species into two occurs. The most likely candidate for such a species is **23**, which could dissociate to give small equilibrium concentrations of arylpalladium halide **18** and monoligated palladium(0) complex **24** (Scheme 7).

Having established the surprising presence of oxidative addition in the rate equation, we continued to establish partial reaction orders for the other reaction components.

3.2.3. Reaction Order in Boronate 19. Next, the partial reaction order in boronate **19** was determined. The partial reaction order with respect to boronate **19** was observed to be 0.89 ± 0.14 (Figure 9). Furthermore, the partial reaction order with respect to boronate **19** was observed to be 0.98 when the experiment was repeated with $[27]_0$ = 1.0 instead of 0.25 M (Supporting Information, page S69).

The experimentally determined partial reaction order of 0.89 ± 0.14 is close to unity, and we assume a first-order rate dependence on the concentration of **19**. Other models can be created to fit the observed data—it is possible that the reaction

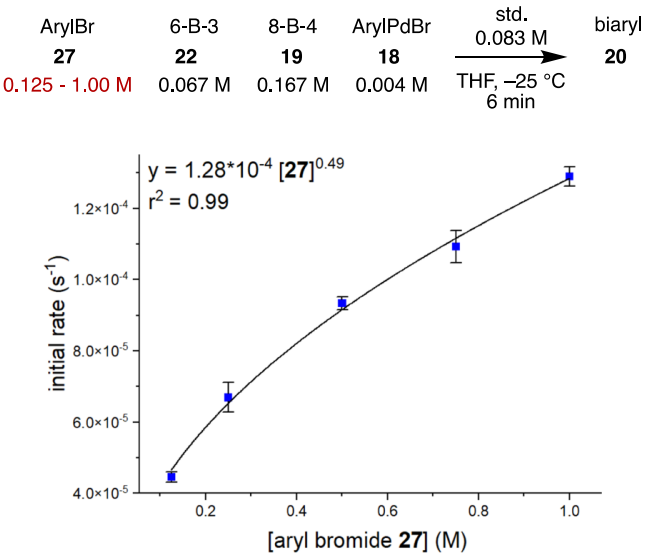

Figure 8. Plot of initial rate vs the concentration of aryl bromide **27**.

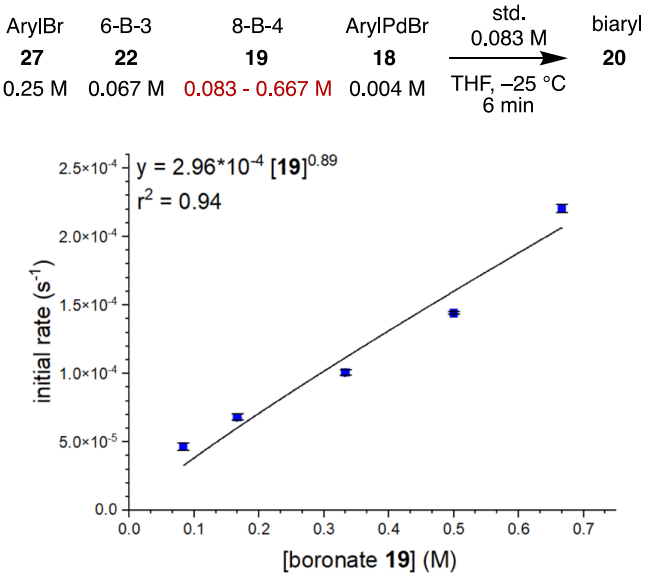

Figure 9. Plot of initial rate vs the concentration of boronate **19**.

order of 0.89 represents the partial saturation of an equilibrium, giving rise to a fractional reaction order or multiple simultaneous mechanisms. Furthermore, the data appear to have a slight upward trend. Two simultaneous reactions, one zeroth-order in **19** and another second-order in **19**, could result in a parabolic rate dependence with a nonzero y-intercept. However, no chemically reasonable hypothesis was imagined as to why such a rate law would be observed. Therefore, it is most appropriate to assume roughly first-order behavior in boronate **19**.

3.2.4. Reaction Order in 6-B-3 Boronic Ester. When the initial rate was measured across a 4-fold range in the concentration of boronic ester **22**, no deviations in the rate were observed (Figure 10). Fitting the data to the power function $y = k_{obs}[22]^a$ reveals that the partial reaction order with respect to 6-B-3 boronic ester **22** is zero.

A zeroth-order dependence on the concentration of boronic ester **22** provides strong evidence against an oxo-palladium (path B) mechanism. In a path B mechanism, 6-B-3 boronic

https://doi.org/10.1021/jacs.1c08283
J. Am. Chem. Soc. 2022, 144, 4345−4364

ArylBr	6-B-3	8-B-4	ArylPdBr	std. 0.083 M	biaryl
27	**22**	**19**	**18**		**20**
0.25 M	0.033 - 0.133 M	0.166 M	0.004 M	THF, −25 °C, 6 min	

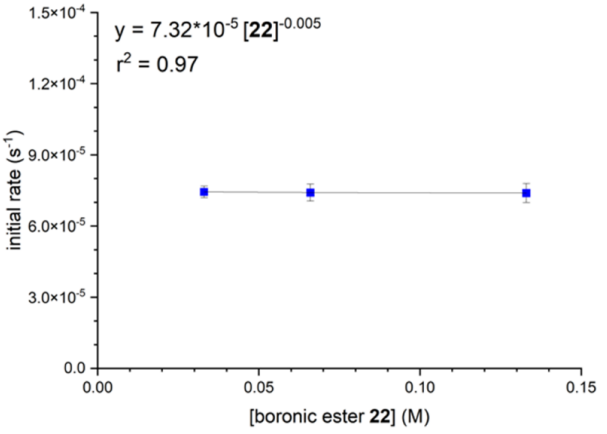

Figure 10. Plot of initial rate vs the concentration of boronic ester **22**.

ArylBr	6-B-3	8-B-4	ArylPdBr	std. 0.083 M	biaryl
27	**22**	**19**	**18**		**20**
0.25 M	0.067 M	0.166 M	0.001 - 0.008 M	THF, −25 °C, 6 min	

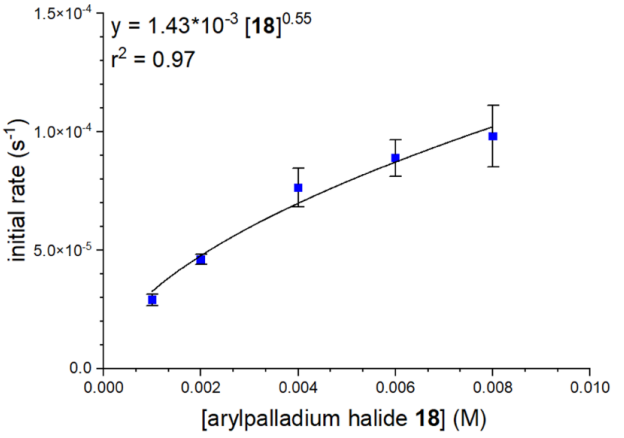

Figure 11. Plot of initial rate vs the concentration of arylpalladium halide **18**.

ester **22** plays two roles, one beneficial and one antagonistic. It is implicated in the transmetalation step, reacting with an arylpalladium−oxyanion complex, but also sequesters the base required to generate an arylpalladium−oxyanion complex. Amatore, Jutand, and Le Duc demonstrate that this dichotomy causes the reaction order in boron species to depend on the concentration of those boron species.[14] However, in Amatore, Jutand, and Le Duc's studies, the reaction order in boronic acid is nonzero at all concentrations of boronic acid. Given the high affinity of TMSOK for boronic esters, the comparatively low affinity of TMSOK for Pd complexes (Section 3.1.6), the zeroth-order partial reaction order in 6-B-3 ester **22**, and the first-order rate dependence on boronate **19**, it is not unreasonable to conclude that transmetalation occurs through a reaction between arylpalladium bromide complex **18** and boronate **19** (path A).

To complete the mechanistic picture, the reaction order in arylpalladium bromide complex **18** was determined.

*3.2.5. Reaction Order in Arylpalladium Halide Complex **18**.* Over an 8-fold range of catalyst concentrations, the reaction order in arylpalladium halide was determined to be 0.55 ± 0.06 (Figure 11).

The observation of a half-order rate dependence on the catalyst concentration is also consistent with a mechanism wherein catalyst disproportionation occurs between the resting state and the turnover-limiting step, in agreement with the partial reaction order in aryl halide **27**.

3.2.6. Summary and Discussion of Kinetic Results. Overall, the kinetic investigations revealed that the reaction is half-order in arylpalladium bromide complex **18**, half-order in aryl bromide **27**, roughly first-order in 8-B-4 complex **19**, and zeroth-order in 6-B-3 boronic ester **22**, resulting in the following rate equation

$$\frac{d[\mathbf{20}]}{dt} = k_{obs}[\mathbf{18}]^{0.55}[\mathbf{27}]^{0.49}[\mathbf{19}]^{0.89} \quad (1)$$

The fractional partial reaction order with respect to **18** and **27** indicates a complex reaction mechanism involving at least one equilibrium. A half-order rate dependence suggests a reversible dissociation of one species into two—the most likely species to fill that role is binuclear complex **23**, particularly given that it is observed in the reaction mixture by ^{19}F NMR spectroscopy (Supporting Information page S21). Four potential mechanisms involving reversible reactions of **23** were considered for the catalytic reaction (Scheme 10). A rate law was derived for each to determine whether the mechanism in question can account for the observed reaction orders. In each of the derivations, there exists a critical bifurcation wherein the rate law depends on the resting state speciation in solution. In general, if the catalytic resting state has at least a moderate concentration of **23**, the reaction will exhibit a half-order rate dependence on the concentration of one or more of the species in solution. If, instead, the resting state palladium species is a mononuclear complex, no fractional reaction orders are observed. A more detailed explanation of this conclusion and a full examination of each rate law are provided in the Supporting Information (pages S110−S130).

The first mechanism (mechanism I) involves reversible oxidative addition of aryl bromide **27** into binuclear complex **23**. The reversibility of oxidative addition in tri-*tert*-butylphosphine ligated palladium complexes has been previously demonstrated by Hartwig and co-workers.[29] The reaction orders predicted for mechanism I depend on the position of the equilibrium **23** + **27** ⇌ 2x **18**. A rate law of $[\mathbf{18}]^{0.5}[\mathbf{27}]^{0.5}[\mathbf{19}]^{1}$ is predicted if the oxidative addition equilibrium favors **23** + **27**, and a rate law of $[\mathbf{18}]^{1}[\mathbf{27}]^{0}[\mathbf{19}]^{1}$ is predicted if the equilibrium favors **18**. The experiments performed herein demonstrate that if such an equilibrium is accessible in our system, it must favor **18**. Arylpalladium bromide complex **18** is observed to be stable in solution and does not spontaneously release aryl halide to form binuclear complex **23**. Furthermore, when **23** and **27** were combined, arylpalladium bromide complex **18** was formed (Section 3.1.5). Because mechanism I requires an equilibrium that favors **23** and **27** to give rise to the experimentally observed reaction orders, it can be ruled out.

The next mechanism considered (II) involves reversible and unfavorable dissociation of **23** into arylpalladium bromide complex **18** and $L_1Pd(0)$ complex **24**. Given that the catalyst

https://doi.org/10.1021/jacs.1c08283
J. Am. Chem. Soc. 2022, 144, 4345−4364

Scheme 10. Four Mechanisms That Were Considered for the Catalytic Reaction

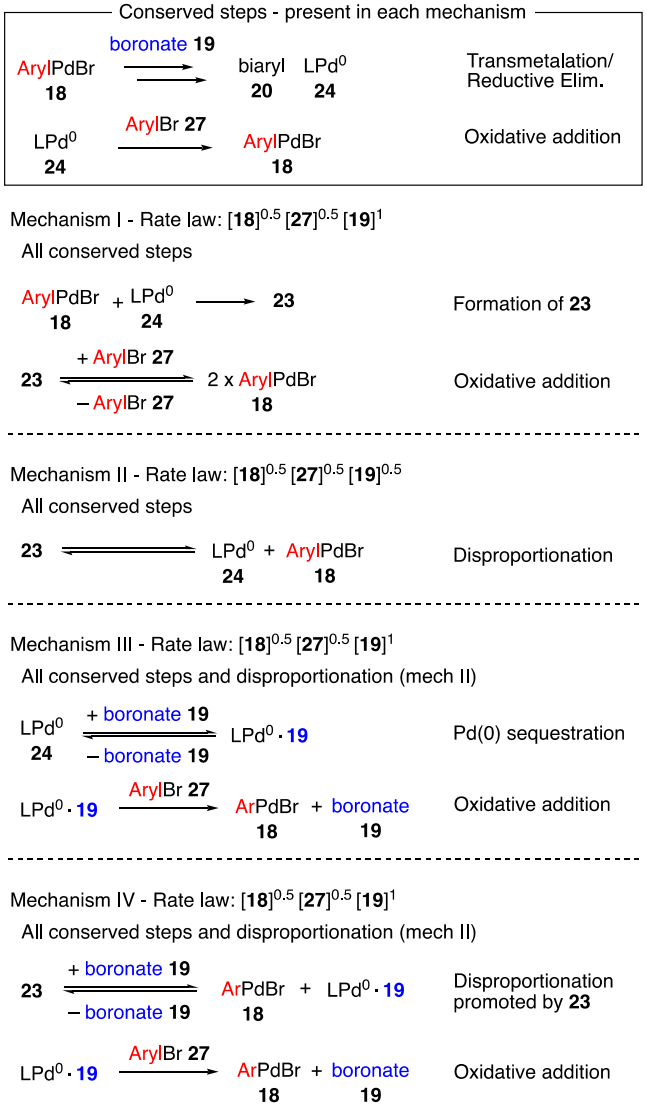

resting state contains **23**, the reaction rate would be proportional to $[\mathbf{18}]^{0.5}[\mathbf{27}]^{0.5}[\mathbf{19}]^{0.5}$—mechanism II does not result in a rate law of $[\mathbf{18}]^{0.5}[\mathbf{27}]^{0.5}[\mathbf{19}]^{1.0}$ under any circumstances. The half-order rate dependence on **27** and **19** arises because oxidative addition and transmetalation each turn over **23** but also creates a species that drives the equilibrium **18** + **24** ⇌ **23** to the right.

A rate law of $[\mathbf{18}]^{0.5}[\mathbf{27}]^{0.5}[\mathbf{19}]^{1}$ can be observed when there are two distinct pathways by which boronate **19** drives the equilibrium **18** + **24** ⇌ **23** to the left. In one such proposed mechanism (III), alongside consuming **18** through transmetalation, boronate complex **19** reversibly binds $L_1Pd(0)$ complex **24** in solution. So long as the resultant complex is still competent to undergo oxidative addition, a reaction rate law of $[\mathbf{18}]^{0.5}[\mathbf{27}]^{0.5}[\mathbf{19}]^{1}$ is possible. Given the coordinatively unsaturated nature of the 12 e^- $L_1Pd(0)$ complex **24**, it is not unreasonable to propose that **24** would bind to **19** to form a new complex.

The data presented herein are consistent with the proposed catalytic cycle shown in Figure 12. However, alternative mechanisms, whereby boronate complex **19** turns over binuclear palladium complex **23** through two distinct pathways, are possible. For example, mechanism IV, wherein boronate complex **19** is implicated in the breakup of the binuclear complex as well as in the transmetalation step, could exhibit a rate law of $[\mathbf{18}]^{0.5}[\mathbf{27}]^{0.5}[\mathbf{19}]^{1}$. The kinetic and stoichiometric data presented herein cannot differentiate between mechanisms III and IV. Furthermore, the proposed complex incorporating **19** and **24** has not been observed or characterized—as such, alternate proposed mechanisms that match all gathered data but do not include **19**·**24** would be equally valid.

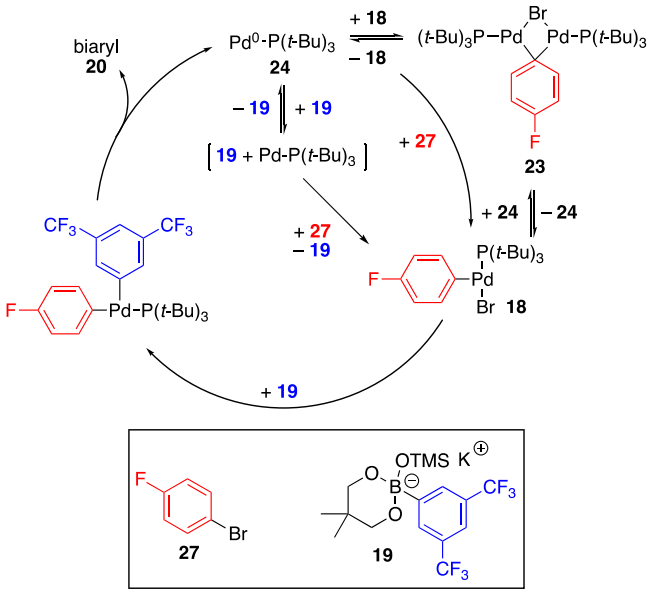

Figure 12. Proposed catalytic cycle for TMSOK-mediated, Suzuki–Miyaura cross-coupling reaction.

Altogether, the lack of observed rate dependence on the concentration of 6-B-3 boronic ester **22**, the positive rate dependence on the concentration of boronate complex **19**, and the observations from studies carried out under stoichiometric conditions strongly support the conclusion that transmetalation takes place through path A, the boronate pathway. The observation of binuclear palladium complex **23** in the reaction mixture by NMR spectroscopy, alongside the half-order dependence in arylpalladium complex **18** and aryl bromide **27**, demonstrates that binuclear palladium complex **23** is more than a curiosity—it is an important intermediate relevant to the catalytic cycle.

Although the use of neopentyl boronic esters as the transmetalating partner and TMSOK as the base differs from "standard" Suzuki–Miyaura reaction conditions, these differences largely affect the transmetalation step. Because transmetalation is not involved in the proposed reaction between $P(t\text{-}Bu)_3Pd(0)$ and $ArylPd[P(t\text{-}Bu)_3]Br$ to form dinuclear palladium complex **23**, it could take place in a significant number of systems. The fundamental difference then may be that very few Suzuki–Miyaura reactions are conducted at −25 °C. With the extraordinary rate of transmetalation observed in this system, the assumption of transmetalation as a turnover-limiting step breaks down, and steps that were previously kinetically silent may become significant.

3.3. Computational Investigation of Binuclear Pd Complex 23. *3.3.1. Introduction.* The discovery of binuclear

https://doi.org/10.1021/jacs.1c08283
J. Am. Chem. Soc. 2022, 144, 4345–4364

Pd complex **23** as a catalytic intermediate was surprising. Although many binuclear Pd(I) complexes are known,[30] no binuclear Pd(I) complex containing a bridging aryl ligand analogous to **23** has been characterized. The only literature precedent is the unligated, binuclear Pd(I) complex **29**, described by Aleksandrov et al. in a computational study of Pd nanoparticle leaching.[31]

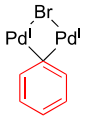

29

Although no μ-phenyl binuclear palladium(I) complex has been experimentally characterized, a limited number of μ-phenyl-bridged binuclear palladium(II) complexes have been characterized, with structures confirmed by X-ray crystallography (Figure 13). The majority of research on μ-phenyl-bridged palladium complexes has focused on the study of **30** through the lens of fundamental inorganic/organometallic chemistry.[32] Analogous complexes such as **31** have been prepared to elucidate when Pd(II) μ-phenyl dimers are stable.[33] Binuclear complex **32** was isolated as an intermediate in the cross-coupling reaction between aryl halides and triarylstibanes.[34] Likewise, binuclear Pd(II) complex **33** was computationally implicated as an intermediate in the Catellani reaction.[35] Finally, binuclear Pd(II) complexes with μ-phenyl bridging ligands have been implicated in the mechanism of Pd-mediated domino reactions[36] and stoichiometric reactions with organotin reagents.[37] Although they are analogous, these Pd(II) binuclear complexes exhibit markedly different reactivity from binuclear Pd(I) complex **23**.

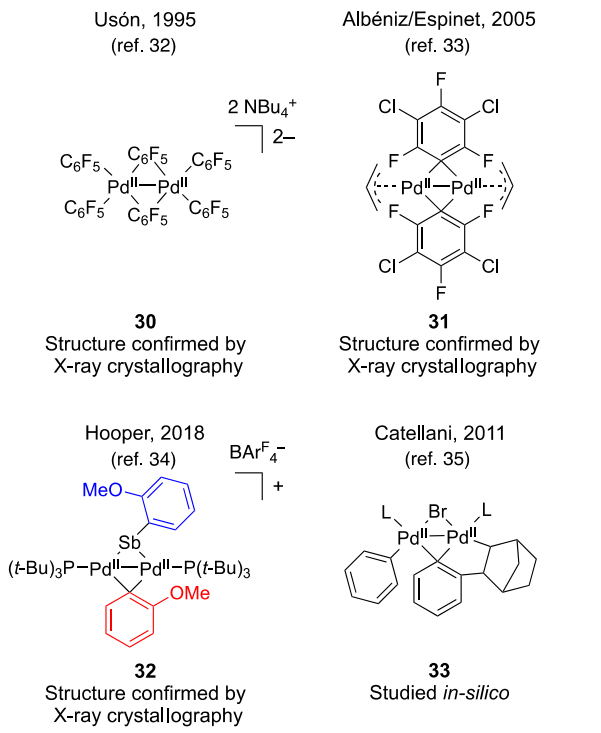

Figure 13. Selected examples of previously described binuclear Pd(II) complexes containing μ-phenyl ligands.

From the literature survey summarized above, it appears that complexes analogous to **23** are thus far unknown. The novelty of complex **23** prompted us to undertake a computational investigation of its structure and bonding. Of particular interest is the geometry of the 4-fluorophenyl ligand, which could conceivably be either a μ-phenyl bridging ligand or a σ-phenyl ligand bound to one palladium center with η^1-coordination to the other palladium center. If the equilibrium geometry were found to contain a σ-phenyl ligand, the complex would need to undergo rapid interconversion to explain the symmetry deduced from the ^{1}H and ^{31}P NMR spectra. Finally, the persistence of a Pd−C−Pd unit in the MS fragmentation led to an investigation into Pd−Pd-bonding interactions in the complex.

3.3.2. Computational Studies. To facilitate the computational investigation of complex **23**, preliminary studies were performed on the model complex **34**, wherein the tri-*tert*-butylphosphine ligands were replaced with trimethylphosphine analogues, and the 4-fluorophenyl substituent was replaced with phenyl for the sake of faster computing time. Calculations were carried out in ORCA 4.2.1 release version.[38] Optimization of the model structure in the singlet state at the *R*PBE[39]/def2-TZVP + ECP(Pd) level of theory showed a strong preference for the unsymmetrical structure **35** with the geometry depicted in Figure 14. The structure did not possess a local C_s symmetry that was anticipated given the experimental NMR chemical shift equivalency of both phosphorus nuclei. The μ^2-aryl group was tilted away from the bisecting plane of Pd−Br−Pd angle (angle Br−C(1)−C(4): 150.3°). The structure obtained at this level of theory can be rationalized chemically as an LPd(0) species utilizing C(1) atom of the LPd(II)(Aryl, Br) oxidative addition fragment as a ligand. When attempts were made to constrain several internal coordinates so that the geometry would resemble the anticipated symmetric structure, a few imaginary modes were obtained, and, upon inspection, one with the phenyl group wagging was identified. Uphill eigenvector following yielded a symmetrical transition state **36**, which again displayed several unexpected geometric features. First, the Br−Pd−C(1)−Pd fragment was significantly puckered, as opposed to being flat, as seen in previously characterized LPd(I)Br dimers (see complexes **37** and **38** in the Supporting information). Second, the Pd−Pd contact elongated by 0.04 Å in the transition state, as compared to the equilibrium structure, potentially indicating a disfavored and avoided Pd−Pd close contact. These observations strongly contradicted the hypothesis of a strong Pd−Pd-bonding interaction.

We hypothesized that the utilization of the restricted Kohn−Sham density functional theory (DFT) theory may be inappropriate for this complex owing to its inability to correctly describe multireference wave functions and decided to obtain a more rigorous picture from a multireference method.[40] Calculations performed at the SA-CASSCF(2,2)[41]/def2-TZVPPD[42] level of theory indicated that both structures **35** and **36** possessed a *significant multireference character*. Even more surprising, the predicted ground electronic state was open shell with a ca. 0.1 eV triplet−singlet splitting in the transition state. These results suggest that the ground-state multiplicity and/or the type of reference wave function was misidentified in the prior calculations. This hypothesis is supported by the propensity of the multireference solution to converge to states with a significant open-shell character. As a result, an optimal geometry was calculated with *U*PBE/def2-TZVP + ECP(Pd) in the high-spin (triplet) state. Beginning with the transition-state geometry **36**, the calculation quickly

https://doi.org/10.1021/jacs.1c08283
J. Am. Chem. Soc. 2022, 144, 4345−4364

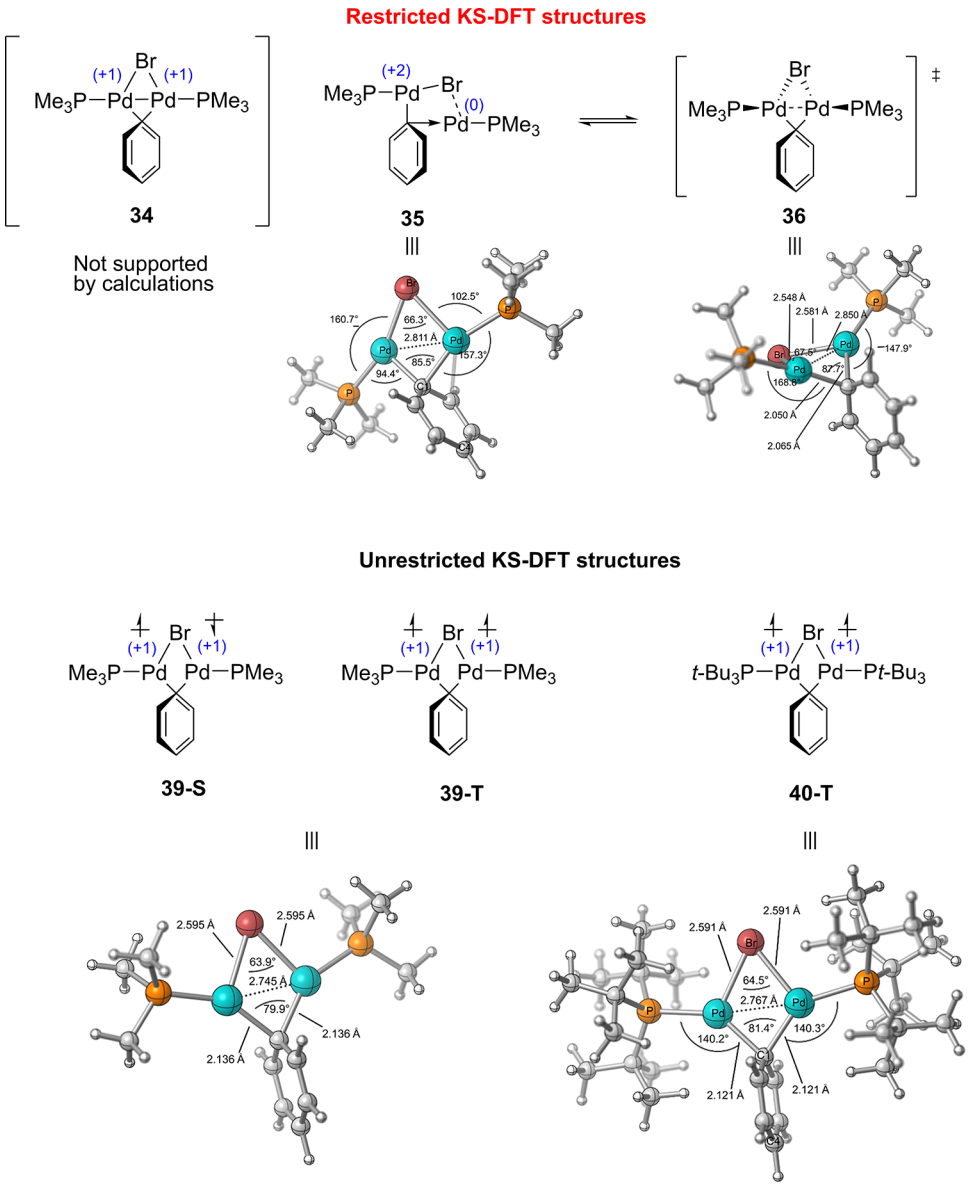

Figure 14. Geometries of computational models and the corresponding electronic structures.

converged on a symmetric structure **39**-T, which had not been observed before. Analytical frequency calculation confirmed that the new structure **39**-T represented a true minimum on the potential energy surface. Attempts to obtain an unrestricted wave function for a singlet electronic state were unsuccessful due to numerical instability.

Application of the SA-CASSCF(2,2)/def2-TZVPPD method to structure **39**-T established that the structure now matched the objective of the DFT optimization: all states were single-determinantal, with the lowest one corresponding to the open-shell triplet state. The symmetry of the structure matched the one deduced from the NMR experiments. Additionally, this epiphany allowed us to rationalize the major mismatch of the structures obtained within RKS and UKS formalism. The effect likely arises from the presence of doubly degenerate, singly occupied nonbonding d-orbitals. Restricted Kohn–Sham orbitals necessitate the double occupancy of one of the two degenerate orbitals, causing a Jahn–Teller effect to emerge. Removal of the orbital degeneracy is possible through a geometry distortion, which results in heavily distorted structures in both the equilibrium and transition states. We believe that both symmetric and distorted geometries are in agreement with each other, once the consequences of orbital degeneracy are taken into account. Optimization of complex **40** at the UKS-DFT level of theory delivered the same symmetric structure. This observation demonstrates that the structural features are general and should be attributed to the electronic structure of the complex, not steric differences between complexes **34** and **40**.

Apart from geometric parameters, the other notable feature of **39**-T is the absence of a direct two-center metallic bonding, as evidenced by the Mayer bond order of 0.22 at the DKH2-FN/*U*PBE/aug-cc-PVTZ-DK level of theory. An alternative possibility for bonding is a three-center four-electron bond. The lowest-energy bonding orbital of this sort is presented in Figure 15a. Analogous explanations for the absence of direct metallic bonding have previously been made for other binuclear palladium complexes.[41,43] We propose that the emergence of this three-centered bond with the μ^2-aryl group, the disappearance of a two-center metallic dσ bond, and the

https://doi.org/10.1021/jacs.1c08283
J. Am. Chem. Soc. 2022, 144, 4345–4364

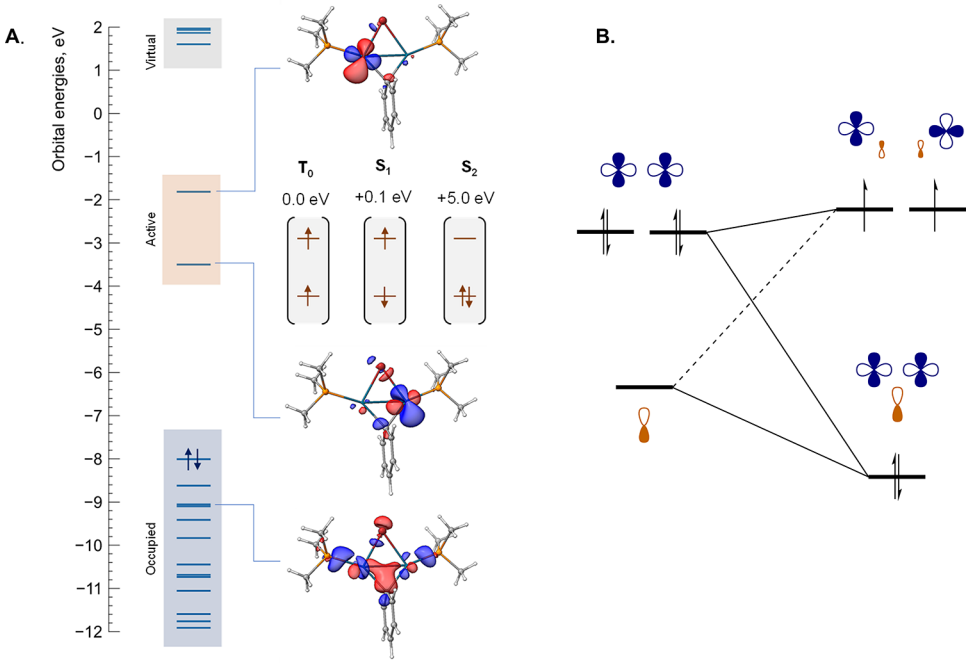

Figure 15. (A) Computed CASSCF orbital energies and occupancies, and the corresponding electronic states. (B) Proposed orbital overlap model to account for open-shell d^9–d^9 structure in **39**.

appearance of the nonbonding unpaired electrons are a result of the strong σ-donor and weak π-acceptor properties of an aryl group. A plausible orbital overlap that could be responsible for this outcome is depicted in Figure 15b. Broken-symmetry DFT calculations were performed to estimate the energy of **39**-S. The calculations support a ferromagnetic coupling between the unpaired electrons, which results in preference for the high-spin (triplet) configuration. The value of magnetic coupling constant (see the Supporting Information) does not appear to be strongly dependent on the percentage of the exact exchange, as hybrid functionals produce similar results to pure generalized gradient approximation (GGA) or meta-GGA functionals. Given that **23** exhibits sharp NMR resonances with unremarkable chemical shift values, we favor the *open-shell singlet* structure of **39**-S as the tentative assignment of the ground electronic structure. It should be noted that the DFT electronic energies of species **35**, **36**, **39-S**, and **39-T** do not align with our conclusions. According to DKH2-PBE calculations, the most stable structure is **35**, followed by **36** (+72.0 kJ mol^{-1}), **39**-T (+83.9 kJ mol^{-1}), and **39**-S (+88.0 kJ mol^{-1}). This disagreement may be explained by the improper treatment of multireference structure within a single-reference DFT formalism. This hypothesis is supported by the CASSCF energies. By comparing the ground-electronic-state energies, one can see that **39**-T is the lowest-energy species, followed by **39**-S (+12.0 kJ mol^{-1}), **35** (+14.5 kJ mol^{-1}), and **36** (+55 kJ mol^{-1}). We cautiously favor the latter energies on the basis of the more consistent electronic structural description, but we refrain from claiming our CASSCF calculations as conclusive in view of the small active space and the absence of dynamic electron correlation.

Although the computational evidence suggests no Pd–Pd bond is present in **23**, a dinuclear palladium species persists following fragmentation in the HCD-MS experiments, suggesting that a Pd–Pd bond might be formed following fragmentation. To investigate further, the same analysis was performed on the cation **41** (Figure 16), a simplified analogue of the key molecular ion in the mass spectrometric analysis (Figure 5). The optimized structure featured the same open-shell ground state as its parent **39**. Unlike the parent structure, cation **41-T** featured a Pd–Pd bond (Mayer bond order of 0.73, DKH2-FN/UPBE/aug-cc-PVTZ-DK). The mass spectrometry data suggest that the metallic bond persists throughout the series of subsequent fragmentations in the mass spectrometer.

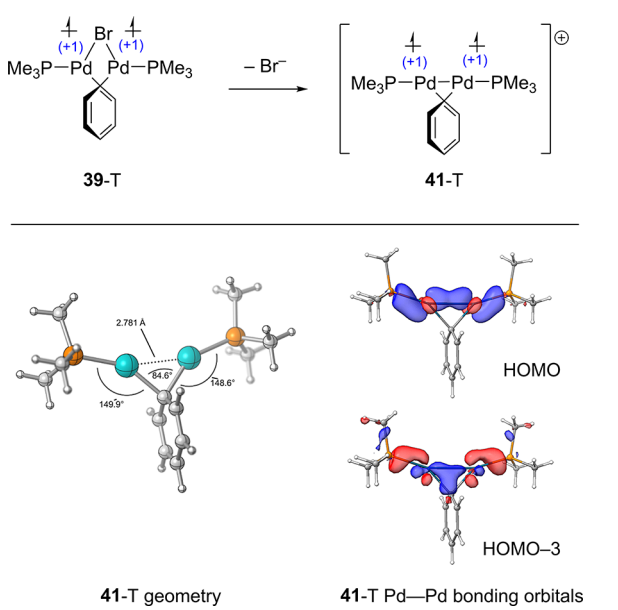

Figure 16. Electronic structure of cation **41**, its geometry, and selected orbitals responsible for Pd–Pd and Pd–C–Pd bonding.

https://doi.org/10.1021/jacs.1c08283
J. Am. Chem. Soc. 2022, 144, 4345–4364

Scheme 11. Analogous Literature Examples in Which Analogues of 23 Were Not Formed, with Proposed Features That Lead to the Absence of 23 Analogues

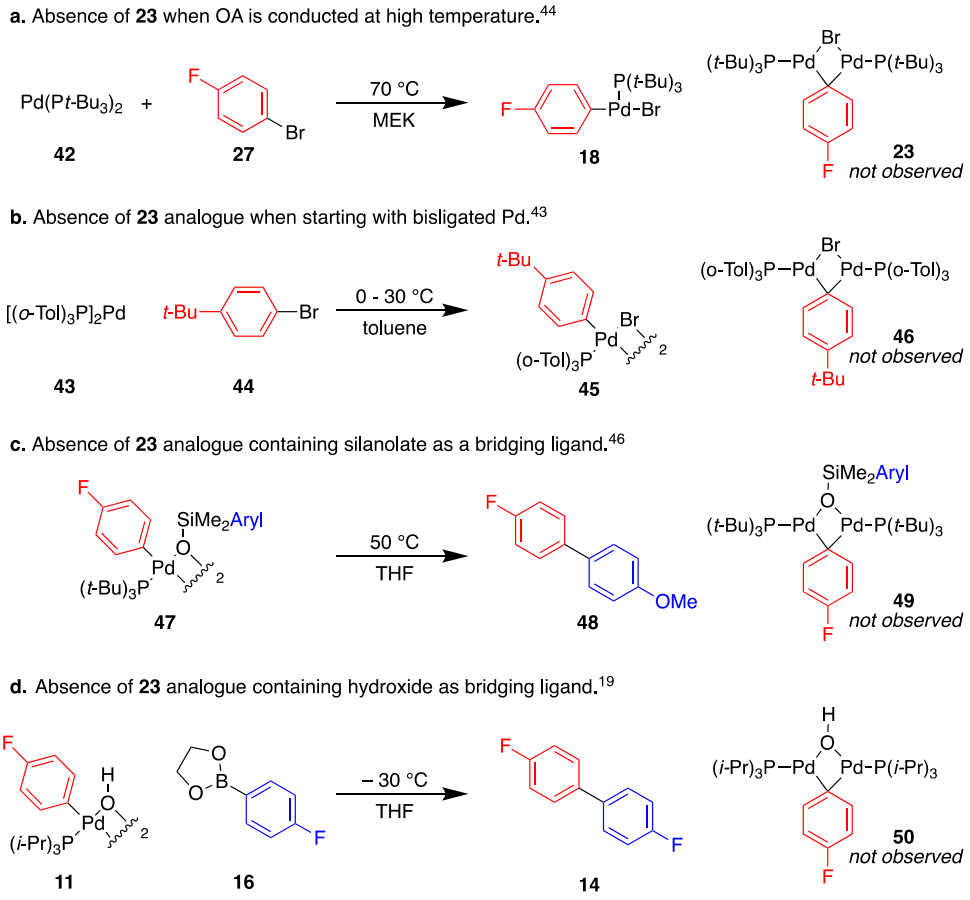

4. DISCUSSION

4.1. Dinuclear Palladium(I) Complex 23. Given the extent to which oxidative addition has been studied, the discovery of a new, related complex is unexpected. The most obvious explanation why such a complex has not been identified is the elevated temperatures generally employed when studying oxidative addition, which may cause rapid decomposition of **23** analogues (Scheme 11a).[44] It is worth noting that oxidative addition to **23** is only slow relative to the rapid transmetalation reaction of TMSOK boronates. If other steps in the catalytic cycle are slow (i.e., in reactions requiring elevated temperatures to proceed at an appreciable rate), other steps may become turnover-limiting, with steps involving **23**-like species becoming kinetically silent.

Another explanation for the absence is the instability of monoligated palladium(0) complexes. Although monoligated palladium(0) complexes are frequently implicated as reaction intermediates through kinetic studies, the reactivity of such complexes has thus far precluded their direct spectroscopic characterization. In general, complexes stabilized by additional phosphine ligands or ligands such as dibenzylideneacetone (dba) are used as precursors to a monoligated palladium(0) complex. Even when conducted at a low (0−30 °C) temperature, no analogue of **23** is observed during oxidative addition reactions of bisligated palladium species (Scheme 11b).[43,45]

It appears that the presence of additional ligands precludes the formation of complexes analogous to **23**. The inability of ArylPd(P*t*-Bu$_3$)Br to dimerize, in contrast with arylpalladium compounds bearing other phosphine ligands, may also play a role. Likewise, other transmetalation reactions of **18** and analogous complexes fail to generate analogues of **23**. It is also hypothesized that the formation of new complexes such as silanolate complex **47** (Scheme 11c) or μ-hydroxide palladium dimer **11** (Scheme 11d) prior to transmetalation precludes the formation of **23** analogues.[19,46]

Complexes analogous to **23** may be relevant intermediates in reactions other than the TMSOK-promoted Suzuki−Miyaura reaction. Precatalysts that generate monoligated palladium(0) species are very useful for palladium-mediated reactions. Because TMSOK and boronic esters are not implicated in the proposed mechanism of formation for **23**, such a complex could be formed in other palladium-mediated reactions of aryl halides starting from monoligated palladium sources, particularly if an arylpalladium halide complex is proposed as the resting state. To summarize, intermediates such as **23** may not always form in Pd-mediated reactions of aryl halides but should be considered when proposing a mechanism for reactions of aryl halides mediated by monoligated palladium(0) in the absence of supporting ligands.

4.2. Lack of Reactivity through Path C. The lack of reactivity through path C can be interpreted in the context of productive reactivity through the boronate pathway or the oxo-palladium pathway. Given our conclusion that the boronate pathway is operative, the lack of reactivity suggests that boronate can displace a halide anion from an arylpalladium(II) complex but cannot displace the silanolate ligand, particularly

https://doi.org/10.1021/jacs.1c08283
J. Am. Chem. Soc. 2022, 144, 4345−4364

when it is present in excess, which disfavors the dissociation of $TMSO^-$ through Le Chatelier's principle. The potential binding of a second molecule of TMSOK to complex **21** (Scheme 6) to form a 10-electron, 5-coordinate silicon complex (10-Si-5) would further inhibit the dissociation of $TMSO^-$. If the oxo-palladium pathway were operative, the lack of free boronic ester that is not bound as the boronate would prevent reactivity, as was described by Amatore, Jutand, and Le Duc.[14] It is notable that similar reaction stalling is observed when potassium *tert*-amylate is used as a homogeneous base in these reactions (Supporting Information, page S12), and analogous effects have been reported in other publications.[47] It follows that, in general, when a homogeneous, anhydrous Suzuki–Miyaura reaction is conducted in the presence of excess base, the reaction may be significantly inhibited by the saturation of both the palladium complex and boron reagent with base.

4.3. Unusual Boronate Transmetalation Mechanism. In view of the longstanding assumption that the oxo-palladium (path B) mechanism is highly preferred for access to the pretransmetalation intermediate, some comment on the demonstration that the boronate pathway (path A) dominates in this process is warranted. In support of the oxo-palladium pathway, Hartwig and Carrow demonstrated that transmetalation from potassium triolboronates is very slow at −40 °C. In contrast, the rate of transmetalation from TMSOK-ligated boronic esters is rapid at −40 °C. Furthermore, previous studies conducted by Amatore, Jutand, and Le Duc demonstrate that reactivity through the oxo-palladium pathway dominates when organic phase-soluble tetrabutylammonium boronates are used as the transmetalating partner.

We hypothesize that in this system, the viability of boronate transmetalation pathway (path A) from TMSOK-complexes of boronic esters is related to the solubility of the potassium boronate and the insolubility of the inorganic salt byproduct, KBr. The solubilized potassium cation could bind as a Lewis acid to the bromide in complexes such as **18**, activating the arylpalladium bromide complex to transmetalation.[48] The tetrabutylammonium cation used in the Amatore/Jutand/Le Duc system would not have the same effect.[49] Likewise, Hartwig and Carrow's use of 18-crown-6 to solubilize potassium boronate salts would inhibit the efficacy of potassium as a Lewis acid.

A possible explanation for a lack of reactivity through the oxo-palladium pathway observed herein is that the high affinity of TMSOK for boron and low affinity for palladium prevent the appropriate speciation to enable that pathway. The observation that ArylPdOTMS complex **21** is poorly defined when generated from a 1:1 mixture of arylpalladium bromide complex **18** and TMSOK supports this hypothesis. Alternatively, an oxo-palladium mechanism would be inhibited if TMSOK cannot effectively serve as a bridging ligand between boron and palladium. An oxo-palladium mechanism would require the initial formation of a Pd–O–B linkage through the -OTMS oxygen, as neopentyl glycol is bound to boron and not free in solution (Scheme 12a). In contrast, the reaction through the boronate pathway allows the more nucleophilic oxygen of neopentyl glycol to act as the bridging ligand (Scheme 12b).

5. CONCLUSIONS

The mechanism of the TMSOK-promoted, anhydrous Suzuki–Miyaura cross-coupling reaction has been elucidated through kinetic analysis and the study of reactivity of isolated reaction intermediates. Stoichiometric studies show that in contrast to prior results, transmetalation through the boronate pathway (path A) can proceed quickly under appropriate reaction conditions. Furthermore, it was demonstrated that the saturation of both palladium and boronate with base (path C) precludes transmetalation, giving rise to base inhibition in homogeneous, anhydrous Suzuki–Miyaura reactions. During the course of the investigation, a novel, binuclear palladium complex containing a μ-arene ligand **23** was characterized and implicated as a catalytic intermediate. Investigation by DFT has demonstrated that complex **23** is an unexpected *open-shell* d^9–d^9 structure that is bound by three-centered four-electron bonds Pd–Br–Pd and Pd–C(1)–Pd. Finally, kinetic analysis supports the conclusion that transmetalation in the catalytic reaction proceeds through the boronate pathway (path A) and implicates **23** in the catalytic reaction mechanism. The findings described herein demonstrate an alternative manifold for the mechanism of the Suzuki–Miyaura cross-coupling reaction under different reaction conditions. The characterization of **23** has mechanistic implications for any reaction of aryl halides catalyzed by a monoligated palladium complex, particularly when an arylpalladium halide complex is proposed as the resting state.

Scheme 12. Implications of the Poor Bridging Ability of -OTMS on the Propensity to React through the Oxo-Palladium and Boronate Mechanisms

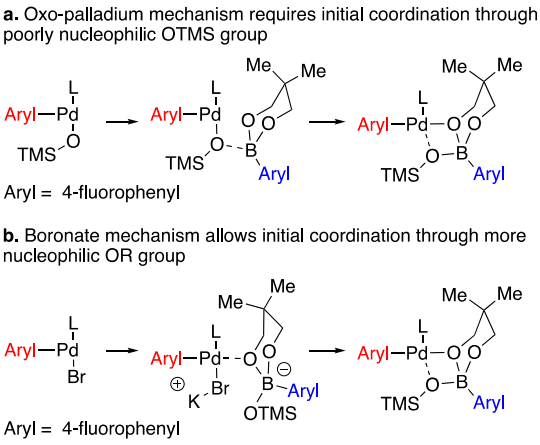

■ ASSOCIATED CONTENT

Supporting Information

The Supporting Information is available free of charge at https://pubs.acs.org/doi/10.1021/jacs.1c08283.

Full experimental procedures and characterization data and copies of ^{1}H, ^{13}C, ^{31}P, ^{19}F, ^{11}B, COSY, HSQC, HMBC, ROESY, and HRMS spectra, along with full kinetic data, rate law derivations and geometries, energies, and coordinates for the calculated structures (PDF)

■ AUTHOR INFORMATION

Corresponding Author

Scott E. Denmark − *Department of Chemistry, University of Illinois at Urbana-Champaign, Urbana, Illinois 61801, United States;* orcid.org/0000-0002-1099-9765; Phone: (217) 333-0066; Email: sdenmark@illinois.edu; Fax: (217) 333-3984

https://doi.org/10.1021/jacs.1c08283
J. Am. Chem. Soc. 2022, 144, 4345−4364

Authors

Connor P. Delaney − *Department of Chemistry, University of Illinois at Urbana-Champaign, Urbana, Illinois 61801, United States;* orcid.org/0000-0002-6885-6011

Daniel P. Marron − *Department of Chemistry, Stanford University, Stanford, California 94305, United States;* orcid.org/0000-0003-1588-768X

Alexander S. Shved − *Department of Chemistry, University of Illinois at Urbana-Champaign, Urbana, Illinois 61801, United States;* orcid.org/0000-0001-5979-179X

Richard N. Zare − *Department of Chemistry, Stanford University, Stanford, California 94305, United States;* orcid.org/0000-0001-5266-4253

Robert M. Waymouth − *Department of Chemistry, Stanford University, Stanford, California 94305, United States;* orcid.org/0000-0001-9862-9509

Complete contact information is available at: https://pubs.acs.org/10.1021/jacs.1c08283

Notes

The authors declare no competing financial interest.

■ ACKNOWLEDGMENTS

The authors are grateful to the National Institutes of Health (GM R35 127010) for generous financial support. The authors thank the Center for Molecular Analysis and Design (CMAD) at Stanford University. R.N.Z. thanks the Air Force Office of Scientific Research through Basic Research Initiative grant (No. AFOSR FA9550-12-1-0400). The authors would like to acknowledge the NMR facility at UIUC for making this study possible, and, in particular, Dr. Lingyang Zhu is thanked for helpful suggestions on NMR spectroscopy. The authors are grateful to Vincent Kassel for operational assistance when running kinetics experiments and to Prof. David Collum (Cornell University) for helpful discussions regarding interpretation of the kinetic results. The authors also thank Prof. Christopher Cramer for helpful discussions regarding the DFT calculations. Dr. Gerald Larson (Gelest) is thanked for generous gifts of TMSOK to support these studies.

■ REFERENCES

(1) Johansson Seechurn, C. C. C.; Kitching, M. O.; Colacot, T. J.; Snieckus, V. Palladium-Catalyzed Cross-Coupling: A Historical Contextual Perspective to the 2010 Nobel Prize. *Angew. Chem., Int. Ed.* **2012**, *51*, 5062−5085.

(2) (a) Krishna, A.; Lunchev, A. V.; Grimsdale, A. C. Suzuki Polycondensation. In *Synthetic Methods for Conjugated Polymers and Carbon Materials*; John Wiley & Sons, Ltd, 2017; pp 59−95. (b) Schlüter, A. D. The Tenth Anniversary of Suzuki Polycondensation (SPC). *J. Polym. Sci. A. Polym Chem.* **2001**, *39*, 1533−1556. (c) Zani, L.; Dessì, A.; Franchi, D.; Calamante, M.; Reginato, G.; Mordini, A. Transition Metal-Catalyzed Cross-Coupling Methodologies for the Engineering of Small Molecules with Applications in Organic Electronics and Photovoltaics. *Coord. Chem. Rev.* **2019**, *392*, 177−236.

(3) (a) Brown, D. G.; Boström, J. Analysis of Past and Present Synthetic Methodologies on Medicinal Chemistry: Where Have All the New Reactions Gone? *J. Med. Chem.* **2016**, *59*, 4443−4458. (b) Roughley, S. D.; Jordan, A. M. The Medicinal Chemist's Toolbox: An Analysis of Reactions Used in the Pursuit of Drug Candidates. *J. Med. Chem.* **2011**, *54*, 3451−3479.

(4) Schiedel, M.-S.; Briehn, C. A.; Bäuerle, P. C−C Cross-Coupling Reactions for the Combinatorial Synthesis of Novel Organic Materials. *J. Organomet. Chem.* **2002**, *653*, 200−208.

(5) (a) Blaser, H.-U.; Indolese, A.; Naud, F.; Nettekoven, U.; Schnyder, A. Industrial R&D on Catalytic C−C and C−N Coupling Reactions: A Personal Account on Goals, Approaches and Results. *Adv. Synth. Catal.* **2004**, *346*, 1583−1598. (b) Corbet, J.-P.; Mignani, G. Selected Patented Cross-Coupling Reaction Technologies. *Chem. Rev.* **2006**, *106*, 2651−2710. (c) Magano, J.; Dunetz, J. R. Large-Scale Applications of Transition Metal-Catalyzed Couplings for the Synthesis of Pharmaceuticals. *Chem. Rev.* **2011**, *111*, 2177−2250.

(6) Nicolaou, K. C.; Bulger, P. G.; Sarlah, D. Palladium-Catalyzed Cross-Coupling Reactions in Total Synthesis. *Angew. Chem., Int. Ed.* **2005**, *44*, 4442−4489.

(7) The Nobel Prize in Chemistry. https://www.nobelprize.org/prizes/chemistry/2010/summary/ 2010 (accessed 2020-04-18).

(8) (a) Miyaura, N.; Yamada, K.; Suzuki, A. A New Stereospecific Cross-Coupling by the Palladium-Catalyzed Reaction of 1-Alkenylboranes with 1-Alkenyl or 1-Alkynyl Halides. *Tetrahedron Lett.* **1979**, *20*, 3437−3440. (b) Miyaura, N.; Suzuki, A. Palladium-Catalyzed Cross-Coupling Reactions of Organoboron Compounds. *Chem. Rev.* **1995**, *95*, 2457−2483. (c) Suzuki, A. Recent Advances in the Cross-Coupling Reactions of Organoboron Derivatives with Organic Electrophiles, 1995−1998. *J. Organomet. Chem.* **1999**, *576*, 147−168. (d) Beletskaya, I. P.; Alonso, F.; Tyurin, V. The Suzuki−Miyaura Reaction after the Nobel Prize. *Coord. Chem. Rev.* **2019**, *385*, 137−173. (e) Pagett, A. B.; Lloyd-Jones, G. C. Suzuki−Miyaura Cross-Coupling. In *Organic Reactions*; John Wiley & Sons, Ltd, 2019; pp 547−620. (f) Lee, J. C. H.; Hall, D. G. State-of-the-Art in Metal-Catalyzed Cross-Coupling Reactions of Organoboron Compounds with Organic Electrophiles. In *Metal-Catalyzed Cross-Coupling Reactions and More*; John Wiley & Sons, Ltd, 2014; pp 65−132.

(9) Echavarren, A. M.; Homs, A. Mechanistic Aspects of Metal-Catalyzed C,C- and C,X-Bond Forming Reactions. In *Metal-Catalyzed Cross-Coupling Reactions and More*; John Wiley & Sons, Ltd, 2013; pp 1−64.

(10) Lennox, A. J. J.; Lloyd-Jones, G. C. Transmetalation in the Suzuki−Miyaura Coupling: The Fork in the Trail. *Angew. Chem., Int. Ed.* **2013**, *52*, 7362−7370.

(11) Matos, K.; Soderquist, J. A. Alkylboranes in the Suzuki−Miyaura Coupling: Stereochemical and Mechanistic Studies. *J. Org. Chem.* **1998**, *63*, 461−470.

(12) Carrow, B. P.; Hartwig, J. F. Distinguishing Between Pathways for Transmetalation in Suzuki−Miyaura Reactions. *J. Am. Chem. Soc.* **2011**, *133*, 2116−2119.

(13) This classification designates N−X−L species, where N is the number of formally valence-shell electrons about atom X, involved in bonding L ligands to X: see Perkins, C. W.; Martin, J. C.; Arduengo, A. J.; Lau, W.; Alegria, A.; Kochi, J. K. An Electrically Neutral σ-Sulfuranyl Radical from the Homolysis of a Perester with Neighboring Sulfenyl Sulfur: 9-S-3 Species. *J. Am. Chem. Soc.* **1980**, *102*, 7753−7759.

(14) Amatore, C.; Jutand, A.; Le Duc, G. Kinetic Data for the Transmetalation/Reductive Elimination in Palladium-Catalyzed Suzuki−Miyaura Reactions: Unexpected Triple Role of Hydroxide Ions Used as Base. *Chem. − Eur. J.* **2011**, *17*, 2492−2503.

(15) Ortuño, M. A.; Lledós, A.; Maseras, F.; Ujaque, G. The Transmetalation Process in Suzuki−Miyaura Reactions: Calculations Indicate Lower Barrier via Boronate Intermediate. *ChemCatChem* **2014**, *6*, 3132−3138.

(16) Lima, C. F. R. A. C.; Rodrigues, A. S. M. C.; Silva, V. L. M.; Silva, A. M. S.; Santos, L. M. N. B. F. Role of the Base and Control of Selectivity in the Suzuki−Miyaura Cross-Coupling Reaction. *ChemCatChem* **2014**, *6*, 1291−1302.

(17) Denmark, S. E.; Williams, B. J.; Eklov, B. M.; Pham, S. M.; Beutner, G. L. Design, Validation, and Implementation of a Rapid-Injection NMR System. *J. Org. Chem.* **2010**, *75*, 5558−5572.

(18) (a) Thomas, A. A.; Denmark, S. E. Pre-Transmetalation Intermediates in the Suzuki−Miyaura Reaction Revealed: The Missing Link. *Science* **2016**, *352*, 329−332. (b) Thomas, A. A.; Wang, H.; Zahrt, A. F.; Denmark, S. E. Structural, Kinetic, and Computational Characterization of the Elusive Arylpalladium(II)-

Boronate Complexes in the Suzuki−Miyaura Reaction. *J. Am. Chem. Soc.* **2017**, *139*, 3805−3821.
(19) Thomas, A. A.; Zahrt, A. F.; Delaney, C. P.; Denmark, S. E. Elucidating the Role of the Boronic Esters in the Suzuki−Miyaura Reaction: Structural, Kinetic, and Computational Investigations. *J. Am. Chem. Soc.* **2018**, *140*, 4401−4416.
(20) (a) Denmark, S. E.; Sweis, R. F. Organosilicon Compounds in Cross-Coupling Reactions. In *Metal-Catalyzed Cross-Coupling Reactions and More*; John Wiley & Sons, Ltd, 2014; pp 475−532. (b) Chang, W.-T. T.; Smith, R. C.; Regens, C. S.; Bailey, A. D.; Werner, N. S.; Denmark, S. E. Cross-Coupling with Organosilicon Compounds. In *Organic Reactions*; John Wiley & Sons, Ltd, 2011; pp 213−746. (c) Denmark, S. E.; Regens, C. S. Palladium-Catalyzed Cross-Coupling Reactions of Organosilanols and Their Salts: Practical Alternatives to Boron- and Tin-Based Methods. *Acc. Chem. Res.* **2008**, *41*, 1486−1499. (d) Denmark, S. E.; Liu, J. H.-C. Silicon-Based Cross-Coupling Reactions in the Total Synthesis of Natural Products. *Angew. Chem., Int. Ed.* **2010**, *49*, 2978−2986.
(21) Delaney, C. P.; Kassel, V. M.; Denmark, S. E. Potassium Trimethylsilanolate Enables Rapid, Homogeneous Suzuki−Miyaura Cross-Coupling of Boronic Esters. *ACS Catal.* **2020**, *10*, 73−80.
(22) Kassel, V. M.; Hanneman, C. P.; Delaney, C. P.; Denmark, S. E. Heteroaryl-Heteroaryl, Suzuki-Miyaura, Anhydrous Cross-coupling Reactions Enabled by Trimethyl Borate. *J. Am. Chem. Soc.* **2021**, *143*, 13845−13853.
(23) (a) Cox, P. A.; Leach, A. G.; Campbell, A. D.; Lloyd-Jones, G. C. Protodeboronation of Heteroaromatic, Vinyl, and Cyclopropyl Boronic Acids: pH-Rate Profiles, Autocatalysis, and Disproportionation. *J. Am. Chem. Soc.* **2016**, *138*, 9145−9157. (b) Cox, P. A.; Reid, M.; Leach, A. G.; Campbell, A. D.; King, E. J.; Lloyd-Jones, G. C. Base-Catalyzed Aryl $B(OH)_2$ Protodeboronation Revisited: From Concerted Proton Transfer to Liberation of a Transient Aryl Anion. *J. Am. Chem. Soc.* **2017**, *139*, 13156−13165. (c) Hayes, H. L. D.; Wei, R.; Assante, M.; Geogheghan, K. J.; Jin, N.; Tomasi, S.; Noonan, G.; Leach, A. G.; Lloyd-Jones, G. C. Protodeboronation of (Hetero)-Arylboronic Esters: Direct versus Prehydrolytic Pathways and Self-/Auto-Catalysis. *J. Am. Chem. Soc.* **2021**, *143*, 14814−14826.
(24) Vikse, K. L.; Woods, M. P.; McIndoe, J. S. Pressurized Sample Infusion for the Continuous Analysis of Air- and Moisture-Sensitive Reactions Using Electrospray Ionization Mass Spectrometry. *Organometallics* **2010**, *29*, 6615−6618.
(25) Yamaguchi, K. Cold-Spray Ionization Mass Spectrometry: Principle and Applications. *J. Mass Spectrom.* **2003**, *38*, 473−490.
(26) Olsen, J. V.; Macek, B.; Lange, O.; Makarov, A.; Horning, S.; Mann, M. Higher-Energy C-Trap Dissociation for Peptide Modification Analysis. *Nat. Methods* **2007**, *4*, 709−712.
(27) Attempts to generate the arylpalladium silanolate complex **21** in THF-H_8 resulted in rapid decomposition of the complex.
(28) Preliminary experiments using Pd-P(*t*-Bu)$_3$-G3 [Buchwald third-generation precatalyst] as the palladium source led to irreproducibility in the initial rate associated with the precatalyst activation step. We believe this observation originates from the comparatively slow rate of the activation of Pd-P(*t*-Bu)$_3$-G3 by TMSOK boronates when compared to free base in solution. For information about Buchwald third-generation precatalysts, see: Bruno, N. C.; Tudge, M. T.; Buchwald, S. L. Design and Preparation of New Palladium Precatalysts for C−C and C−N Cross-Coupling Reactions. *Chem. Sci.* **2013**, *4*, 916−920.
(29) (a) Roy, A. H.; Hartwig, J. F. Reductive Elimination of Aryl Halides from Palladium(II). *J. Am. Chem. Soc.* **2001**, *123*, 1232−1233. (b) Roy, A. H.; Hartwig, J. F. Directly Observed Reductive Elimination of Aryl Halides from Monomeric Arylpalladium(II) Halide Complexes. *J. Am. Chem. Soc.* **2003**, *125*, 13944−13945. (c) Roy, A. H.; Hartwig, J. F. Reductive Elimination of Aryl Halides upon Addition of Hindered Alkylphosphines to Dimeric Arylpalladium(II) Halide Complexes. *Organometallics* **2004**, *23*, 1533−1541.
(30) Inatomi, T.; Koga, Y.; Matsubara, K. Dinuclear Nickel(I) and Palladium(I) Complexes for Highly Active Transformations of Organic Compounds. *Molecules* **2018**, *23*, 140.
(31) Zvereva, E. E.; Katsyuba, S. A.; Dyson, P. J.; Aleksandrov, A. V. Leaching from Palladium Nanoparticles in an Ionic Liquid Leads to the Formation of Ionic Monometallic Species. *J. Phys. Chem. Lett.* **2017**, *8*, 3452−3456.
(32) (a) Usón, R.; Forniés, J.; Tomás, M.; Casas, J. M.; Navarro, R. Synthesis and Reactivity of Binuclear Homo- or Hetero-Metallic Complexes $[NBu_4]_2[MM'(\mu\text{-}C_6F_5)_2(C_6F_5)_4]$ (M = M′= Pd or Pt; M = Pt, M′= Pd) with Bridging Pentafluorophenyl Groups. *J. Chem. Soc., Dalton Trans.* **1989**, *1*, 169−172. (b) Usón, R.; Forniés, J.; Tomás, M.; Martínez, F.; Casas, J. M.; Fortuño, C. Symmetric or Unsymmetric Cleavage of the Bridging System in $[M_2(\mu\text{-}C_6F_5)_2(C_6F_5)_4]^{2-}$ (M_2 = Pt_2, Pd_2 or PtPd) with 2,2′-Bipyridine or 1,10-Phenanthroline. Molecular Structure of $[PPN]_2[(C_6F_5)_3Pt(\mu\text{-}Bpy)Pt(C_6F_5)_3]$ and $[NBu_4][Pt(C_6F_5)_3(Phen)]$. *Inorg. Chim. Acta* **1995**, *235*, 51−60. (c) Casas, J. M.; Falvello, L. R.; Forniés, J.; Mansilla, G.; Martín, A. Synthesis and Structural Characterization of Platinum and Palladium Complexes Containing O-Donor $C_6X_2O_4^{2-}$ Ligands. *Polyhedron* **1998**, *18*, 403−412.
(33) Albéniz, A. C.; Espinet, P.; López-Cimas, O.; Martín-Ruiz, B. Dimeric Palladium Complexes with Bridging Aryl Groups: When Are They Stable? *Chem. − Eur. J.* **2005**, *11*, 242−252.
(34) Simpson, Q.; Sinclair, M. J. G.; Lupton, D. W.; Chaplin, A. B.; Hooper, J. F. Oxidative Cross-Coupling of Boron and Antimony Nucleophiles via Palladium(I). *Org. Lett.* **2018**, *20*, 5537−5540.
(35) Maestri, G.; Motti, E.; Della Ca', N.; Malacria, M.; Derat, E.; Catellani, M. Of the Ortho Effect in Palladium/Norbornene-Catalyzed Reactions: A Theoretical Investigation. *J. Am. Chem. Soc.* **2011**, *133*, 8574−8585.
(36) Cárdenas, D. J.; Martín-Matute, B.; Echavarren, A. M. Aryl Transfer between Pd(II) Centers or Pd(IV) Intermediates in Pd-Catalyzed Domino Reactions. *J. Am. Chem. Soc.* **2006**, *128*, 5033−5040.
(37) Albéniz, A. C.; Espinet, P.; Martín-Ruiz, B. The Pd-Catalyzed Coupling of Allyl Halides and Tin Aryls: Why the Catalytic Reaction Works and the Stoichiometric Reaction Does Not. *Chem. − Eur. J.* **2001**, *7*, 2481−2489.
(38) (a) Neese, F. Software Update: The ORCA Program System, Version 4.0. *Wiley Interdiscip. Rev.: Comput. Mol. Sci.* **2018**, *8*, No. e1327. (b) Neese, F. The ORCA Program System. *Wiley Interdiscip. Rev.: Comput. Mol. Sci.* **2012**, *2*, 73−78.
(39) Cramer, C. J.; Truhlar, D. G. Density Functional Theory for Transition Metals and Transition Metal Chemistry. *Phys. Chem. Chem. Phys.* **2009**, *11*, 10757−10816.
(40) Ayed, T.; Guihéry, N.; Tangour, B.; Barthelat, J.-C. Theoretical Study of the Metal−Metal Interaction in Dipalladium(I) Complexes. *Theor. Chem. Acc.* **2006**, *116*, 497−504.
(41) Rappoport, D.; Furche, F. Property-Optimized Gaussian Basis Sets for Molecular Response Calculations. *J. Chem. Phys.* **2010**, *133*, No. 134105.
(42) Kostic, N. M.; Fenske, R. F. Molecular Orbital Study of Dinuclear Palladium Carbonyl Chlorides. Choice of the Bridging Ligand (Carbonyl vs. Chloro) and the Question of Metal-Metal Bonding. *Inorg. Chem.* **1983**, *22*, 666−671.
(43) Hartwig, J. F.; Paul, F. Oxidative Addition of Aryl Bromide after Dissociation of Phosphine from a Two-Coordinate Palladium(0) Complex, Bis(Tri-o-Tolylphosphine)Palladium(0). *J. Am. Chem. Soc.* **1995**, *117*, 5373−5374.
(44) Carrow, B. P.; Hartwig, J. F. Ligandless, Anionic, Arylpalladium Halide Intermediates in the Heck Reaction. *J. Am. Chem. Soc.* **2010**, *132*, 79−81.
(45) (a) Galardon, E.; Ramdeehul, S.; Brown, J. M.; Cowley, A.; Hii, K. K.; Mimi; Jutand, A. Profound Steric Control of Reactivity in Aryl Halide Addition to Bisphosphane Palladium(0) Complexes. *Angew. Chem., Int. Ed.* **2002**, *41*, 1760−1763. (b) Barrios-Landeros, F.; Hartwig, J. F. Distinct Mechanisms for the Oxidative Addition of Chloro-, Bromo-, and Iodoarenes to a Bisphosphine Palladium(0)

https://doi.org/10.1021/jacs.1c08283
J. Am. Chem. Soc. 2022, 144, 4345−4364

Complex with Hindered Ligands. *J. Am. Chem. Soc.* **2005**, *127*, 6944–6945.
(46) Tymonko, S. A.; Smith, R. C.; Ambrosi, A.; Ober, M. H.; Wang, H.; Denmark, S. E. Mechanistic Significance of the Si–O–Pd Bond in the Palladium-Catalyzed Cross-Coupling Reactions of Arylsilanolates. *J. Am. Chem. Soc.* **2015**, *137*, 6200–6218.
(47) Wethman, R.; Derosa, J.; Tran, V. T.; Kang, T.; Apolinar, O.; Abraham, A.; Kleinmans, R.; Wisniewski, S. R.; Coombs, J. R.; Engle, K. M. An Under-Appreciated Source of Reproducibility Issues in Cross-Coupling: Solid-State Decomposition of Primary Sodium Alkoxides in Air. *ACS Catal.* **2021**, *11*, 502–508.
(48) Beutner, G. L.; Coombs, J. R.; Green, R. A.; Inankur, B.; Lin, D.; Qiu, J.; Roberts, F.; Simmons, E. M.; Wisniewski, S. R. Palladium-Catalyzed Amidation and Amination of (Hetero)Aryl Chlorides under Homogeneous Conditions Enabled by a Soluble DBU/NaTFA Dual-Base System. *Org. Process Res. Dev.* **2019**, *23*, 1529–1537.
(49) Interestingly, under the reaction conditions employed by Amatore, Jutand, and Le Duc, the presence of alkali cations inhibits the rate of reaction because the alkali metals bind to the arylpalladium hydroxide complex implicated in transmetalation through the oxo-palladium pathway. Amatore, C.; Jutand, A.; Le Duc, G. Mechanistic Origin of Antagonist Effects of Usual Anionic Bases (OH^-, CO_3^{2-}) as Modulated by their Countercations (Na^+, Cs^+, K^+) in Palladium-Catalyzed Suzuki-Miyaura Reactions. *Chem. – Eur. J.* **2012**, *18*, 6616–6625.

https://doi.org/10.1021/jacs.1c08283
J. Am. Chem. Soc. 2022, 144, 4345–4364